universität wien

MASTERARBEIT / MASTER'S THESIS

Titel der Masterarbeit / Title of the Master's Thesis

„Development of a metabolomics method for the investigation of a case of apparent symbiosis"

verfasst von / submitted by

Yasin El Abiead BSc

angestrebter akademischer Grad / in partial fulfilment of the requirements for the degree of

Master of Science (MSc)

Wien, 2017 / Vienna 2017

Studienkennzahl lt. Studienblatt / degree programme code as it appears on the student record sheet:	A 066 862
Studienrichtung lt. Studienblatt / degree programme as it appears on the student record sheet:	Chemie
Betreut von / Supervisor:	Univ.-Prof. Dr. Gunda Köllensperger

Acknowledgements

There are a number of people without whom I would not have been able to perform this work as it is presented here.

First of all, I would like to thank my supervisor Gunda Köllensperger for her guidance and the opportunities she gave me to improve my abilities and follow my ideas. Special thanks go to Michaela Schwaiger and Evelyn Rampler who never hesitated to help with practical problems and were always available to discuss funny ideas. My sincere thanks are also going to the rest of the working group as everybody was participating to the friendly and constructive working atmosphere that allowed me to look forward to every single working day. Additionally, I want to thank Petra Pjevac from our cooperation partners, who did her best to explain the biological context of my study to me.

Last but not least, I want to say that I am very grateful to my mother who supported me through my whole (quite long) education process and beyond.

Abstract

Metabolomics is a rapidly developing research field with many different possible applications with the aim to identify and quantify small molecules. However, there are still many unsolved issues and pitfalls that restrict its potential in terms of reliability and explorative use. Within the presented work some of those topics were broached within the frame of a metabolomics study. To put it into biological context targeted and untargeted metabolomics approaches were utilised to investigate an apparent symbiosis between the ammonia oxidising archaea *Nitrosospharea gargensis* and a betaproteobacterium. For the sake of this, monocultures as well as a co-culture of the organisms of interest were probed. In order to explore the samples as comprehensive as possible, the technical advantages of high resolution mass spectrometry and different orthogonal separation techniques, namely high performance reversed phase chromatography and anion exchange chromatography were applied. Moreover, absolute quantification of a number of targeted analytes was achieved by the use of yeast-extracted ^{13}C labelled internal standards.

As limits of detection for small organic molecules are becoming lower and lower, contaminations are becoming more and more an issue. This is especially true for untargeted metabolomics where contamination can easily be misinterpreted for sample components or lead to other problems like ion suppression. In order to become more aware of the extensiveness of this problem, the contamination potential of a number of lab materials was investigated.

Zusammenfassung

Bei Metabolomics handelt es sich um ein sich schnell entwickelndes Forschungsgebiet, das in vielen Bereichen Anwendung findet. Allerdings gibt es noch immer viele ungelöste Probleme die verhindern, dass das volle Potential der Forschungsrichtung, hinsichtlich Verlässlichkeit und Aufklärung ausgeschöpft werden kann. In der hier vorliegenden Arbeit wurden einige dieser Punkte im Rahmen einer metabolomischen Studie thematisiert. Dafür wurde die scheinbare Symbiose zwischen der Ammonium oxidierenden Archaea *Nitrosospharea gargensis* und Betaproteobakterien sowohl mit einer gezielten als auch einer ungezielten metabolischen Analyse untersucht, wobei sowohl Monokulturen als auch Co-Kulturen der beiden Organismen beprobt wurden. Um alle Proben so umfassend wie möglich analysieren zu können wurden die technischen Vorzüge von hochauflösender Massenspektrometrie und unterschiedlicher zueinander orthogonaler Trenntechniken genutzt. Bei den Trenntechniken handelte es sich um Umkehrphasen-Hochleistungsflüssigchromatographie und Anionenaustauschchromatographie. Außerdem wurden einige Analyten unter Zuhilfenahme von, aus Hefe extrahierten, ^{13}C markierten internen Standards absolut quantifiziert.

Da die Nachweisgrenzen für kleine organische Moleküle immer geringer werden, spielen Kontaminationen eine immer größere Rolle. Dies gilt besonders für ungezielte Metabolomics Ansätze, bei denen Kontaminationen leicht für Probenkomponenten gehalten werden können. Darüber hinaus können Kontaminanten auch zu anderen Problemen, wie zum Beispiel Ionensuppression, führen. Um die Tragweite dieses Problems besser abschätzen zu können, wurde das Kontaminierungspotential einiger im Labor verwendeter Gegenstände untersucht.

Table of contents

1 Introduction

1.1 The roots of metabolomics

Already in the 1960s, the measurement of metabolites via mass spectrometry became an established routine (Anggard and Sedvall, 1969; Schwartz et al., 1967). However, in this time most metabolic studies were related to the identification of drugs and their metabolites. Only in 1998 Oliver et al. proposed to determine metabolites and their relative concentrations for systems biology purposes (e.g. reversed genetics) (Oliver et al., 1998). It was in 2000 when Fiehn et al. first used the term “metabolomics” (Fiehn et al., 2000a). Later, he also pointed out that metabolites are giving the fastest responses to genetic or environmental changes on the molecular level (Fiehn, 2002). Not only those scientific motivations but certainly also the improvements in instrumentation over the time (especially mass spectrometry and chromatography) increased the interest in metabolomics during the following years.

1.2 Subdivisions of metabolomics

The field of metabolomics can be divided into two major subdivisions, namely targeted and untargeted metabolomics. Both of them hold different approaches and workflows to obtain qualitative and quantitative information about the metabolome (**Figure 1**). A detailed description of different approaches addressing the two tasks is given elsewhere (Fiehn, 2001).

1.2.1 Targeted Metabolomics

Targeted analysis always involves the quantification of targeted analytes utilising external calibration (B. Dunn et al., 2005; Dettmer et al., 2007). However, in order to achieve a precise and accurate quantification, internal standards (ideally isotopically labelled 13C metabolites of interest (Lehmann, 2017; Neubauer et al., 2012a, 2012b)) have to be added to all samples and standards in the same concentration as one of the first sample preparation steps. This is necessary to correct any error accumulated in the analytical chain of sample preparation and measurement such as analyte degradation or recovery. Moreover, ionisation sources like electrospray ionisation (ESI) cannot be stable over a whole measurement series (Editors). By internal standardisation it is possible to

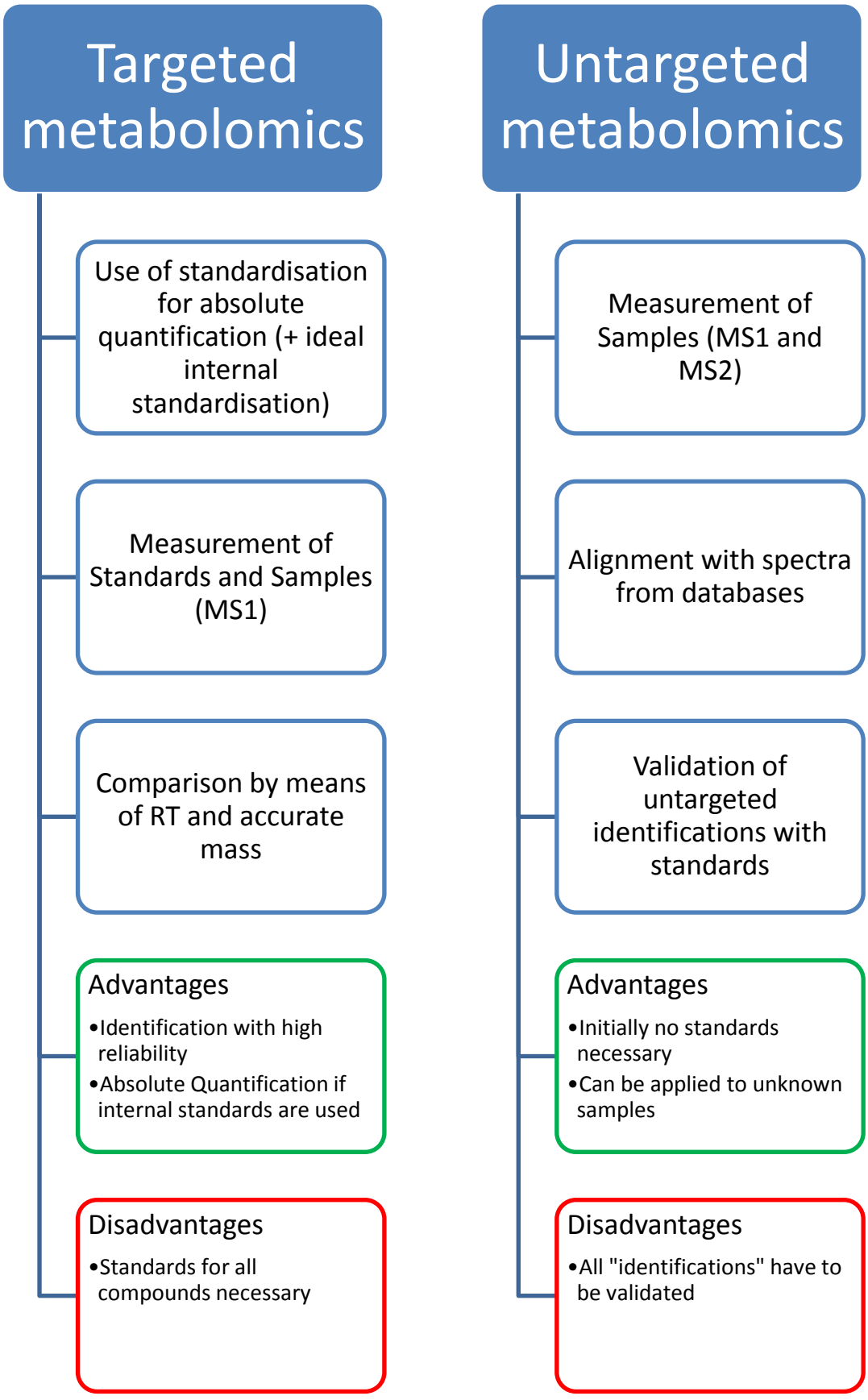

Figure 1 Simplified workflow, advantages and disadvantages of targeted/untargeted metabolomics

correct those fluctuations. Hence, internal standardisation is crucial for reliable quantification approaches (Neubauer et al., 2012a). In a nutshell, targeted metabolomics is an approach that offers reliable identification and quantification of metabolites. However, only components with commercially available standards can be analysed. This means, targeted analysis is only applicable to identify analytes being specifically searched for but is not capable of analysing completely unknown samples.

1.2.2 Untargeted Metabolomics

On the other hand, untargeted metabolomics uses a different approach. Initially, there is no need for standards, as compounds are identified by comparing their accurate mass and MS2 spectra with compound libraries or databases like mzCloud (MS2 spectra and exact masses) or ChemSpider (exact masses) (Theodoridis et al., 2011). However, the reliability of identifications generated this way will always be restricted not only by the similarity of the fragmentation spectra of some compounds, but also because of the fact that databases simply do not contain all compounds. Hence, if the database being used does not contain a substance, an algorithm might incorrectly identify the component with the next best match. Additionally, there are also other reasons for mismatches such as differences in instrumental parameters or other experimental conditions influencing fragmentation. Consequently, identifications generated by untargeted metabolomics always have to be validated by standards. The metabolomics society defined quality levels of compound identification (Sumner et al., 2007):

(1) Identified compounds – at least two independent and orthogonal data have to be reported (e.g. retention time (RT) and mass spectrum)
(2) Putatively annotated compounds – those are based only on physicochemical properties and/or spectral similarities with spectra from the very same compound from spectral libraries
(3) Putatively characterised compound classes – in comparison to the second level spectra and/or physicochemical properties of analytes are only compared to those of compounds of the same compound-class here
(4) Unknown compounds – features that remain unclassified but can be observed as a peak

1.3 Testing for significance

Statistical and mathematical techniques are becoming more and more crucial in metabolomics. For example, they are needed in order to assess significance and relevance of differences in concentration (Franceschi et al., 2013; Ortmayr et al., 2015), to carry out multi-parameter optimisations of liquid chromatography-MS (LC-MS) methods (Rhoades and Weljie, 2016) and for simplification of complex multidimensional data (Fiehn et al., 2000a; Taylor et al., 2002). The evaluation of the significance of differences between two sample groups is one of the most common statistical tasks that has to be met by scientists in the field of metabolomics (Shellie et al., 2005). Especially for the identification of biomarkers, which is a key competence of metabolomics, testing of significance is indispensable (Preez et al., 2017; Roy et al., 2004). The common procedure for significance evaluation is to test the so-called null hypothesis H_0, which is that the values of a normally distributed variable do not depend on predefined sample groups. Before this can be done, each metabolite should be checked for normality. One commonly used test is the so-called Lilliefors test (Conover, 1999). If a metabolite in one of the investigated sample groups fails the test, a non-parametric test like the Mann-Whitney U test has to be performed in order to assess a possible significant difference. Alternatively, it can be tried to transform a non-normal distribution into a normal one by transformations such as logarithmic transformations (Broadhurst and Kell, 2006). Within this work all distributions are assumed to be normal. Under this assumption, H_0 can be tested with different test statistics which are, in case of the commonly used t-test, leading to a p-value. That value is a measure of the probability of getting a result as extreme or extremer than observed in the grab sample if H_0 is true and can therefore reach values between 0 and 1. H_0 is discarded at a confidence interval of $1 - \alpha$ if the p-value falls under a predefined significance level α (often 0.05 or 0.01, which would lead to a probability of 5% and 1% respectively of wrongly rejecting H_0). However, when this approach, which is intended for the use on single variables separately, is applied to *–omics* datasets the so-called "multiple-testing problem" arises. There are two different ways to tackle this problem. One is to control the family-wise error rate, which strives for the idea that if two sample groups are not different, none of their variables should be different (and is therefore very restrictive). The other strategy is to control the false discovery rate (FDR) (basic concept from Benjamini and Hochberg (Benjamini and Hochberg, 1995)) in a way that less true positives (truly different variables) are lost which comes at the price of accepting a

reasonable fraction of false positives. As this strategy was also used in this work, it will be explained in more detail. A description of how to control the family-wise error rate and other possibilities to control the FDR are given elsewhere (Franceschi et al., 2013). The method proposed by Benjamini and Hochberg requires that the *m* p-values are put in an ascending sequence {$p_1 \ldots p_m$} (Benjamini and Hochberg, 1995). Then the FDR is controlled in a way that it stays below a chosen fraction q^* within the set of found positives. Finally, *k* is the largest *i* for which

$$p_i \leq \frac{i}{m} q^* \qquad \textbf{Equation 1}$$

and all null hypothesis $H_0(1) - H_0(k)$ are rejected. Hence, a new higher significance level α is chosen to correct for the multiple-testing effect. However, there is also the possibility to adjust the p-value directly so that the initial thresholds can still be applied. In case of the Benjamini Hochberg approach, again the ordered list of p-values is used and the adjusted p-values $\tilde{p}$s are given by

$$\tilde{p}_{j_{k=j\ldots m}} = \left(\min\left(p_k \frac{m}{k}, 1\right)\right). \qquad \textbf{Equation 2}$$

It should be noted that $\tilde{p}$s are not real estimates of any kind of probability anymore. Additionally, it is possible to take into account correlated variables. In metabolomics examples of such correlated variables could be signals corresponding to different adducts or in-source fragments of the same molecule if implications of the ESI are considered. Naturally, it is also promising to take biological information like pathways into account. However, as this technique was not applied in the present work, it is therefore not further discussed. A closer description on this topic is given elsewhere (Franceschi et al., 2013). However, the t-test as discussed until now can only be applied if exactly two different groups are compared. In case of more than two groups the so-called one-way analysis of variance (ANOVA) can be utilised. Actually, the t-test is just a special case of ANOVA where the number of groups equals two. Generally spoken, ANOVA is forming a ratio F between the variance estimated from sample means and the variance within the samples. Therefore, a higher F value implies that the investigated samples were drawn from more than one population. However, in order to find out which of the groups are different to each other, some “post-hoc” analysis has to be carried out. That kind of analysis tests which means are significantly different from each other and leads to a p-value. One of those tests, which was also used in the here

presented work, is the so-called Tukey's honest significant difference (Tukey HSD) test (Tukey, 1949). This test basically works like a t-test with additional control of the family-wise error rate.

1.4 Elucidation of molecular formulas

It is within the nature of untargeted metabolomics that the elemental composition of analysed compounds is not known initially. In order to elucidate the total formula, seven rules have been established and critically evaluated by Kind and Fiehn (Kind and Fiehn, 2007):

(1) Element numbers should be restricted in order to save computational time. This can be done roughly by dividing the highest expected exact molecule mass through the accurate mass of the element in question (assuming only singly charged ions in case of molecules < 1000 Da).
(2) Determined molecular formulas need to be checked for their physical existence. This is done utilizing the LEWIS and the SENIOR rule. In general, the LEWIS rule applies to all molecules. However, there are some like free radicals and several hypervalent molecules (Noury et al., 2002) which could not exist according to the LEWIS rule. If such molecules need to be checked, the SENIOR rule can be utilised.
(3) The isotopic pattern of the various elements utilizing the natural abundances of their isotopes needs to be taken into account (Kind and Fiehn, 2006). This adds a valuable orthogonal measure to the accurate mass of an analyte that can be used for validation purposes (Sumner et al., 2007).
(4) For most compound classes an H/C – ratio between 0.1 and 6 can be assumed.
(5) Moreover, heteroatom ratio thresholds can be used to restrict the search space.
(6) In rule (5) only individual element ratios are checked. However, it is also unlikely that a high number of different heteroatoms occurs, which is therefore factored in in rule (6).
(7) The last rule indicates that in case of derivatised analytes or adducts, the original molecular formula needs to be determined before the other rules can be applied. The necessary number of derivatised groups that need to be subtracted can easily be calculated, if the derivatisation reagent incorporates elements with a notably isotopic pattern as it has already been shown for trimethylsilyl groups (Fiehn et al., 2000b).

Naturally, the same strategy could be applied to other groups containing elements with a striking isotopic pattern like Br.

An important requirement that has to be met in order to be able to use most of these rules is to measure with sufficient mass accuracy, resolving power and isotopic pattern accuracy. However, the mere force of high mass accuracy should not be overestimated, as even at a theoretical accuracy of 0.1 ppm only molecules with masses < 185.9760 Da could be assigned unambiguously (Kind and Fiehn, 2006). The importance of mass resolving power is in general depending on the complexity of the sample. However, usually it is not known whether there are mass interferences that could not be resolved with a given resolution. Therefore, it is advisable to go always for the highest mass resolution possible. This is not only because some components might not be distinguishable at poor resolution, but also due to the fact that unresolved mass spectral peaks lead to a poor mass accuracy which does not meet the mass precision anymore (G. Marshall et al., 2013; Marshall et al., 2002). Some signals might therefore not be assignable to any molecular formula anymore which can lead to the loss of some or all parenting compounds for further analysis.

1.5 Identification of unknown compounds

In order to be able to interpret an MS-signal within a biological context it is necessary to identify the actual molecule related to it. With reference to Sumner *et al.* (Sumner et al., 2007) it is enough to compare a sample compound with a standard by means of two independent physicochemical properties in order to label it as identified. By this means, the accurate mass and isotopic pattern would already be sufficient as stated earlier. However, it is also recommended to validate identifications by additional orthogonal physicochemical parameters as RT and MS2 spectra comparison (Sumner et al., 2007). Actually, it would not be possible to achieve unambiguous identifications without that additional data as a molecular formula could usually be matched to more than one molecule in a database. The generation of MS2 spectra is therefore indispensable for identification purposes.

1.5.1 Maximizing identifications

In an untargeted analysis it is usually one of the main targets to be as comprehensive as possible. Due to the limitation of ionisation sources regarding ion suppression, the chimeric MS2-spectra generation due to quadrupole-isolation (Lawson et al., 2017) and the presence of isobaric and isomeric compounds among other reasons, a prior separation technique (e.g.

chromatography) is required. This is for obvious reasons especially important for the analysis of low concentrated compounds in the presence of high concentrated compounds as it is very common in biological samples (B. Dunn et al., 2005). However, classic high performance liquid chromatography (HPLC) methods still do not lead to the metabolome coverage desired by many scientists. Hence, there are many examples in literature where researchers try to improve those separations or change other instrumental or chemical parameters to maximize the coverage of the metabolome. Some of those approaches are to improve the chromatographic separation (Ortmayr et al., 2016; Rainville et al., 2014), the ionisation process (Yanes et al., 2011) or the tuning parameters of the mass spectrometer (Ranninger et al., 2016). One of the attempts of Ranninger *et al.* was to split the mass scan range in order to optimize the ionisation parameters for the low mass range (50-200 m/z) and the high mass range (200 – 1000 m/z) individually. However, they met the problem that they could not optimize the tuning parameters in the low mass range in a way that does not increase the background signals disproportionally high. Yet, they did not report any attempt to lower that background (Ranninger et al., 2016). Therefore, one of the aims of this work is to find ways to decrease it.

1.6 Biological task

Only in 2005 the existence and importance of ammonia oxidizing archaea (AOA) was first described by Könneke et al. (Könneke et al., 2005). Three years later, a moderately thermophilic and chemolithoautotrophic AOA, "*Candidatus Nitrosospharea gargensis*" was described and subsequently isolated in pure culture (Hatzenpichler et al., 2008; Palatinszky et al., 2015). Later on, a bacterium capable of conducting the whole nitrification-cascade (from ammonium over nitrite to nitrate – (comammox)) in one step and another AOA were identified, cultured and described (Daims et al., 2015; Lebedeva et al., 2013). What all those nitrifying microbes had in common was that a bacterium affiliated to the class *Betaproteobacteria* was present in the respective enrichment cultures. However, the reason for this apparent symbiosis is still unknown. In order to get to the bottom of this interaction, the betaproteobacterium and one representative of AOA (*Nitrosospharea gargensis*) were cultivated in different monocultures and as co-culture. As it was not possible to derive the interaction in question by mere investigation of the isolated genomes, a multi-omics approach was utilised. The idea was to merge the knowledge about the genome of the organism with proteomics and metabolomics data. Within this frame, proteomics had the

task of providing information about the presence of enzymes in the studied organisms. The expected interaction between the microorganisms is based on an exchange of molecules with the cell supernatant acting as transitional medium. Hence, metabolites in the supernatant were investigated employing a metabolomics approach. From the genomic (the genome of the betaproteobacterium was published in Daims et al. 2015 (Daims et al., 2015)) and proteomic data (unpublished data) some target analytes could be deduced. The full list of target analytes is shown in **Table 1**. In a previous study, investigating interactions of ammonia oxidizing bacteria (AOB) with heterotrophic microorganisms, Sedlacek and colleagues (Sedlacek et al., 2016) found that eight proteins involved in amino acid synthesis are significantly decreased in an AOB when it is grown in co-culture with heterotrophic bacteria. Other authors showed that this AOB actually encodes two amino acid transporters in their genome (Bollmann et al., 2013) and previous work showed an increased growth rate when amino acids were present in their medium (Clark and Schmidt, 1967; Frijlink et al., 1992). As consequence, all amino acids were put on the targeted list. Within the genome of the betaproteobacterium, genes encoding for a methanol dehydrogenases and other alcohol dehydrogenases were found. Proteomic data showed these dehydrogenases were expressed in enrichment cultures containing the betaproteobacterium and the comammox organism, *Nitrospira inopinata* (unpublished data). Ectoin and hydroxyectoine are two protectants against heat stress, which the betaproteobacterium should be able to produce according to their genome. Hence, the hypothesis of the betaproteobacterium releasing those protectors into the medium, so that the AOA can subsequently benefit from them, was tested too. Therefore, both protectors were added to the target list. Cobalamin can be produced by various archaea (Doxey et al., 2015; Rodionov et al., 2003) and is known to be released into the environment as part of a symbiosis by some microorganisms like AOAs, as it is an essential cofactor (Sañudo-Wilhelmy et al., 2014). At last, α-keto acids (pyruvate and oxaloacetate) were shown to counteract the toxicity of hydrogen peroxide which is produced by AOAs during ammonia oxidation (Kim et al., 2016). Hence, pyruvate and oxaloacetate were added to the target list for the sake of testing the hypothesis of α-keto acids being produced by betaproteobacterium for the benefit of AOAs.

Table 1 List of metabolites which were arguably interesting for quantification and subsequently investigated within the present study.

Target substances			
Alanine	Glutamine	Lysine	Pyruvate
Arginine	Glutamic acid	Methanol[a]	Serine
Asparagine	Glycine	Methionine	Threonine
Aspartic acid	Histidine	Methylamine	Tryptophan
Cobalamin[a]	Hydroxyectoine	Oxaloacetate[a]	Tyrosine
Cysteine[a]	Isoleucine	Phenylalanine	Valine
Ectoine	Leucine	Proline	

a) Cobalamin, methanol, cysteine and oxaloacetate have not been investigated within this study due to unsolved issues.

2 Methods

2.1 Sample preparation

2.1.1 Cell culture samples

Samples from Set A were prepared by the cooperation partner at the faculty of biology at the University of Vienna. There were five different sample groups with supernatants of different bacteria cultures (5 biological replicates each) which are listed in the following as "prokaryote name (supplement substrates; abbreviation)": *Nitrososphaera Gargensis* (6 mM ammoniumchloride; G), betaproteobacteria (6 mM acetate; BA), betaproteobacteria (6 mM thiosulfate; BT), betaproteobacteria (6 mM methanesulfonic acid; BM) and *N. Gargensis* & betaproteobacteria (6 mM ammoniumchloride; BG). Each culture was sampled once at the end of its exponential growth phase (T1) and once in its stationary growth phase (T2). Additionally, one biological replicate of each sample group was prepared by freezing the cells in order to destroy their membrane and subsequently filtering them. This was done in order to create a sample that can be used to check whether cell leakage during filtration of the cells that have not been frozen prior to filtration can be excluded. The ingredients of the media other than the supplement substrates are listed in **Table 2**. In order to obtain the supernatants, bacteria were removed utilizing a syringe filter (pore size 0.1 µm; polyethersulfone). Another sample was prepared by filtration of fresh media. After sampling, a 13C-labeled yeast extract was added to some technical replicates of each sample (v/v, 1/20) for internal standardisation purposes, while others were left without for the sake of untargeted analysis.

Table 2 The pH (8) of the media was adjusted with HCl, NaOH and $NaHCO_3$. Consequently the concentrations of Na^+ and Cl^- can be slightly different from the given concentrations.

Main components	**Concentration [g/L]**
KH_2PO_4	0.05
KCl	0.075
$MgSO_4 \times 7H_2O$	0.05
NaCl	0.584
$CaCO_3$	0.01-1.00
Trace elements	**Concentration [µg/L]**
$MnSO_4 \times H_2O$	34.4
H_3BO_3	50.0
$ZnCl_2$	70.0
$Na_2MoO_4 \times 2H_2O$	72.6
$CuCl_2 \times 2H_2O$	20.0
$NiCl_2 \times 6H_2O$	24.0
$CoCl_2 \times 6H_2O$	80.0
$FeSO_4 \times 7H_2O$	1000
$Na_2SeO_3 \times 5H_2O$	3.0
$Na_2WO_4 \times 2H_2O$	4.0

2.1.2 Contamination samples

Samples for this experiment were prepared in order to tackle the problem of high background in the low mass range. Therefore different samples were prepared with three replicates each:

- Five different vial types were analysed (Thermo Fisher Scientific Chromacol™ vials (TC), Thermo Fisher Scientific National™ MS-certified pre-cleaned vials with sliced and unsliced pre-cleaned caps (TN41 and TN35 respectively), Macherey Nagel GmbH vials (MN), Lab Logistic Group GmbH vials which were heated to 500°C overnight a few days previous to analysis (stored in aluminium foil in the meantime) (H)). For

their preparation no pipets were used. Additionally special care was taken that the solvents did not come in direct contact with the caps:

- Vials were directly filled with LC-MS grade water out of the bottle.
- Vials were washed three times with LC-MS grade water before filling with LC-MS grade water for analysis.
- Vials were washed three times with LC-MS grade methanol and three times with LC-MS grade water before filling with LC-MS grade water for analysis.
- Vials were directly filled with LC-MS grade water out of the bottle and closed. Then they were shaken for 1 min so that the eluent comes into harsh contact with the cap (only done with vials from MN).
- Vials were directly filled with LC-MS grade water out of the bottle and closed with sliced caps. Then they were shaken for 1 min so that the eluent comes into harsh contact with the cap (only done with vials from MN).

- 1.5 mL plastic tubes (Eppendorf Tubes® 3810X) and 15 mL centrifuge tubes (Eppendorf) were analysed. For their preparation no pipets were used. All tubes were extracted for 42 h with LC-MS grade water in the fridge. For analysis some of it was transferred into vials from MN.
  - Tubes were directly filled with LC-MS grade water out of the bottle.
  - Tubes were washed three times with LC-MS grade water before filling with LC-MS grade water for analysis.
  - Tubes were washed three times with LC-MS grade methanol and three times with LC-MS grade water before filling with LC-MS grade water for analysis.

- The potential influence of different gloves (Nitrile gloves from Star Lab, SHIELD Scientivic and Kimtech and rubber gloves from Budexx; all gloves were powder-free) was investigated. Therefore, three squares (for three replicates) of 1 cm^2 each were cut out of each glove and extracted with LC-MS grade water in MN vials for 1 min.

- Pipette tips from Eppendorf (200 µL and 1000 µL), Greiner Bio-One (200 µL) and Star Lab (200µL and 1000 µL) were investigated. For the extraction LC-MS grade water

was pipetted into vials from MN. While pipetting the water was left in the pipet for approximately 3 s. With each tip the maximum volume was pipetted.

2.2 Measurements

All measurements were carried out on a high resolution mass spectrometer (Orbitrap Q Exactive HF, Thermo Scientific).

2.2.1 Cell culture experiments

2.2.1.1 Preparation of the multi-component standard (MCS)

Initially each compound was dissolved separately either in water (pyruvate (Pyr)), 0.1 M HCl (asparagine (Asn), cysteine (Cys), glutamate (Glt), glutamine (Glu), glycine (Gly), serine (Ser), alanine (Ala), aspartate (Asp), lysine (Lys), proline (Pro), threonine (Thr), tyrosine (Tyr), ectoine (Ect) and hydroxyectoine (Hec)), 0.1 M HCOOH (methionine (Met), valine (Val), arginine (Arg), histidine (His), isoleucine (Ile), leucine (Leu) and phenylalanine (Phe)) or 0.1 M NaOH (tryptophan (Trp)). After full dissolution they were mixed and brought to concentrations of 50 µM each. From this stock solution a 10 µM calibration standard was prepared containing a 13C-labeled yeast extract for internal standardisation purposes. All further dilutions were conducted with water. For external calibration purposes 10 additional calibration standards (5000, 2500, 1250, 1000, 500, 250, 125, 63, 31 and 16 nM) were produced by dilution of the produced 10 µM standard.

2.2.1.2 Reversed phase chromatography – separation method

For reversed-phase (RP) separation a silica based column (Waters Acquity HSS T3, 2.1 × 150 mm, 1.8 µm particle size) was used. The flow rate was set to 0.3 mL/min at a temperature of 40 ± 0.5°C. The chromatographic run (**Table 3**) was started with 2 min of 100% mobile phase A (99.9% water, 0.1% formic acid) followed by a linear gradient to 40% mobile phase B (100% methanol) in 4 min and another linear gradient to 100% mobile phase B in 2 min. Those conditions were maintained for 3 min. Then the column was re-equilibrated for another 4 min with 100% mobile phase A. Hence, the overall runtime was 15 min. The injection volume was 10 µL. Every ten samples a pooled sample (consisting of a mixture of multiple samples), a quality control (1250 nM standard) and a blank were injected.

Table 3 The gradient of the reversed phase (RP) method is given in this table. Mobile phase A consisted of 99.9% water and 0.1% formic acid. Mobile phase B consisted of 100% methanol.

Time [min]	Mobile phase A [%]	Mobile phase B [%]
0	100	0
2	100	0
6	60	40
8	0	100
11	0	100
11.1	100	0
15	100	0

2.2.1.3 Anion exchange chromatography – separation method

For anion exchange (IC) the separation was conducted on a Dionex Integrion HPIC System, from Thermo Scientific, equipped with a Dionex IonPac AS11-HC column (Thermo Scientific, 2 × 50 mm, 4 µm particle size). The flow rate was set to 0.38 mL/min at a temperature of 30°C in the column oven. The chromatographic run (**Table 4**) was started with 10 mM NaOH during the first three minutes of the method, followed by a linear gradient to 50 mM NaOH which it reached in the twelfth minute of the chromatographic method. Within the next five minutes the NaOH concentration was linearly elevated to 100 mM and held at this level for four minutes. From minute 21.0 to minute 21.1 the NaOH concentration was decreased again to 10 mM and held at this level until the end of the chromatographic run. Hence, the whole method lasted for 25 minutes. The injection volume was 5 µL. Every ten samples a pooled sample (consisting of a mixture of multiple samples), a quality control (1000 nM standard) and a blank were injected.

2.2.1.4 Mass spectrometry – method

Each sample was analysed in positive and negative ion mode (IC samples only negative). The Full MS-method employed an m/z range of 60 – 900, a mass resolution of 60000, an automatic gain control (AGC) of 1E6 and a maximum fill time (MFT) of 100 ms. For another Full MS / data dependent (dd)-MS2 method the AGC target was changed to 3E6 and the MFT to 50 ms for Full MS. The dd-MS2-properties were set to a resolution of 15000, an AGC target of 1E5, a MFT of 30 ms and an isolation window of 1.6 m/z. The minimum AGC target was set to 1000.

Table 4 The gradient of the ion exchange chromatography (IC) method is given in this table.

Time [min]	NaOH concentration [mM]
0	10
3	10
12	50
17	100
21	100
21.1	10
25	10

2.2.2 Contamination experiments

All contamination experiments were conducted with the RP chromatography separation method as described above. However, no quality control, blanks or pooled samples were applied. Moreover, the different replicates have been measured set wise (at first one replicate of each sample group, then the second ones and in the end the third ones). The MS-method was utilised as before.

2.3 Data evaluation

In case of the cell culture experiments the aim of this work was to use the data generated by the established LC-MS method to identify metabolites within the supernatants which can possibly give indications for interactions between *N. Gargensis* and the betaproteobacteria. In order to obtain this objective targeted (Thermo Scientifics *Tracefinder 3.3*) and untargeted (Thermos *Compound Discoverer 2.0*) metabolomics approaches were utilised.

2.3.1 Untargeted Metabolomics

For the untargeted processing of the recorded data *Compound Discoverer 2.0* (CD) was used. On the single mass spectra level no intensity threshold was introduced. For the RT alignment a mass tolerance of 3 ppm and a maximum RT shift of 0.3 min were allowed. A feature was accepted when its minimum peak intensity exceeded a threshold of 1E5 counts*s^{-1} and a minimum of seven scans per peak. Additionally, a minimum number of 2 isotopes had to be found by the software for every compound in order to be listed as such. For the inter sample grouping of the unknown compounds the mass tolerance was set to 3 ppm and a RT shift up to 0.15 min was allowed. Moreover a CD-node called “Fill Gaps” was used. This node operated in a way that whenever a compound was detected in at least one sample the

applied intensity thresholds were ignored for all the other samples within the applied RT and mass tolerance limits. However, even if there was no mass trace at all a small integration was performed so that there were no non-detects left in the end. Those non-detect values are typically below 1E4 counts*s^{-1}. Hence, this value was used as a threshold on many occasions within the present work. For the MS2 spectra comparison mzCloud was utilised. Therefore a precursor mass tolerance of 5 ppm was used.

2.3.1.1 Report of untargeted data

Different diagrams were used in order to report untargeted data. Naturally, different filters have to be applied to the features found by the feature-extraction algorithms of the untargeted software in order to set up the various diagrams. In the present study, mainly principal component analysis (PCA) and Venn diagrams (VD) have been applied. For the PCAs only features that were present with a peak area of at least 1E4 counts*s^{-1} in all replicates of at least one sample group with a feature coefficient of variance (FV%) of less than 50% were considered. Although the threshold of 1E4 counts*s^{-1} is kind of arbitrary it's necessary to utilise such a threshold as the Fill gaps function of CD was always integrating a peak even if no signal is visible in the mass trace at all. Additionally, all replicates had to exceed the threshold as the sample size was quite small (5 and 3 for the cell culture studies and the contaminant studies respectively), which can easily lead to false positives due to artefacts. For the VD features had to exceed an area intensity threshold of 1E4 counts*s^{-1} in each replicate and a FV% of less than 50% in order to be counted as present in a sample group. Additionally, an in-house Microsoft Excel macro was used to find features shared between different groups. In order for features to be considered to be related to the same compound the mass difference had to be less than 6 ppm and the RT difference had to be less than 0.3 min. If a feature with the same mass (± 6 ppm) was present more than once within this RT window it was counted only once. This is due to problems of the feature-extraction software which is often considering single peaks as more than one peak. Although it would make sense to correct for this before any untargeted data interpretation it was only done for the VD within this study because it would arguably introduce the biggest error there. Recently a freely available tool capable of taking this and other problems like misinterpretation of contaminants into account was recently published by DeFelice *et al.* (DeFelice et al., 2017).

2.3.2 Targeted metabolomics

Calibration was performed using the MCS with eleven different concentrations as described before. For each measured compound in each measured sample five calibration points (out of eleven) were chosen to be taken into account for the linear regression model of the calibration line. Those five points were chosen in an automatized way by an in-house Microsoft Excel macro. This was done in a way that for the signal of each compound in each individual sample the calibration points with the next higher and next lower signal were selected. In addition to those two points three other calibration points were chosen in a way that the sum of the square roots of the residuals of the two points is reaching the lowest value possible. For each possible combination of those three points three different weighing factors ($1/x^{1/2}$, $1/x$ and $1/x^2$) were tested (Almeida et al., 2002) additionally to the unweighted linear regression in order to check whether the residual square roots can be minimised even further. The five points leading to the best result are then used with the according regression model to get the slope k and intercept d of the calibration line. Samples with signals higher or lower than those of the highest respectively lowest standard signal were not considered by the macro.

3 Results and Discussion

3.1 Cell culture experiments

3.1.1 Signal stability of the measurements

All targeted compounds were investigated in positive as well as in negative ion mode as $[M+H]^+$ adducts and $[M-H]^-$ ions respectively. For positive ion mode the variability-coefficient of calculated concentrations stayed below 6% for almost all compounds in the QC sample and the pooled sample for which internal standardisation could be used (**Figure 2** and **Figure 3**). Exceptions were glycine and lysine, with 35% and 13% respectively. For lysine, which eluted close to the dead volume, a possible explanation is the formation of other adducts in competition with $[M+H]^+$ as can be seen in **Figure 5**. This is due to the fact that the salt concentration of the sample matrix was quite high (see **Table 2**) and salts are generally eluting within the dead volume of a reversed phase column. From the same figure it can be seen that not only lysine was competing for Na^+ and K^+ ions in order to form adducts, but also other components within the dead volume. This becomes obvious when a closer look is given to the total ion chromatogram (TIC). Only when the majority of the dead volume compounds eluted from the column, Na^+ and K^+ adducts started to form also with lysine which leads to a drop in intensity of the $[M+H]^+$ signal. Overall the area of the shown salt adducts accounts for 23% of all observed lysine signals shown. In consequence of the mentioned points, already small RT shifts, changes in peak width or a slightly different matrix composition or concentration can theoretically lead to major differences in the observed signal intensity of one of the lysine adducts. In case of glycine, the area of the salt adducts accounts for even 30% of all observed glycine signals in the given example. Also in this case, it is conceivable that the absence or presence of other molecules might enhance or suppress the formation of other adducts than $[M+H]^+$. However, regarding electrospray ionisation glycine is known to be problematic in general.

3.1.2 Recovery of used filters

The recovery of used filters was tested with one of the calibration standards for all targeted analytes. However, no effect of the filter on any of the targeted analytes could be found (**Figure 4**).

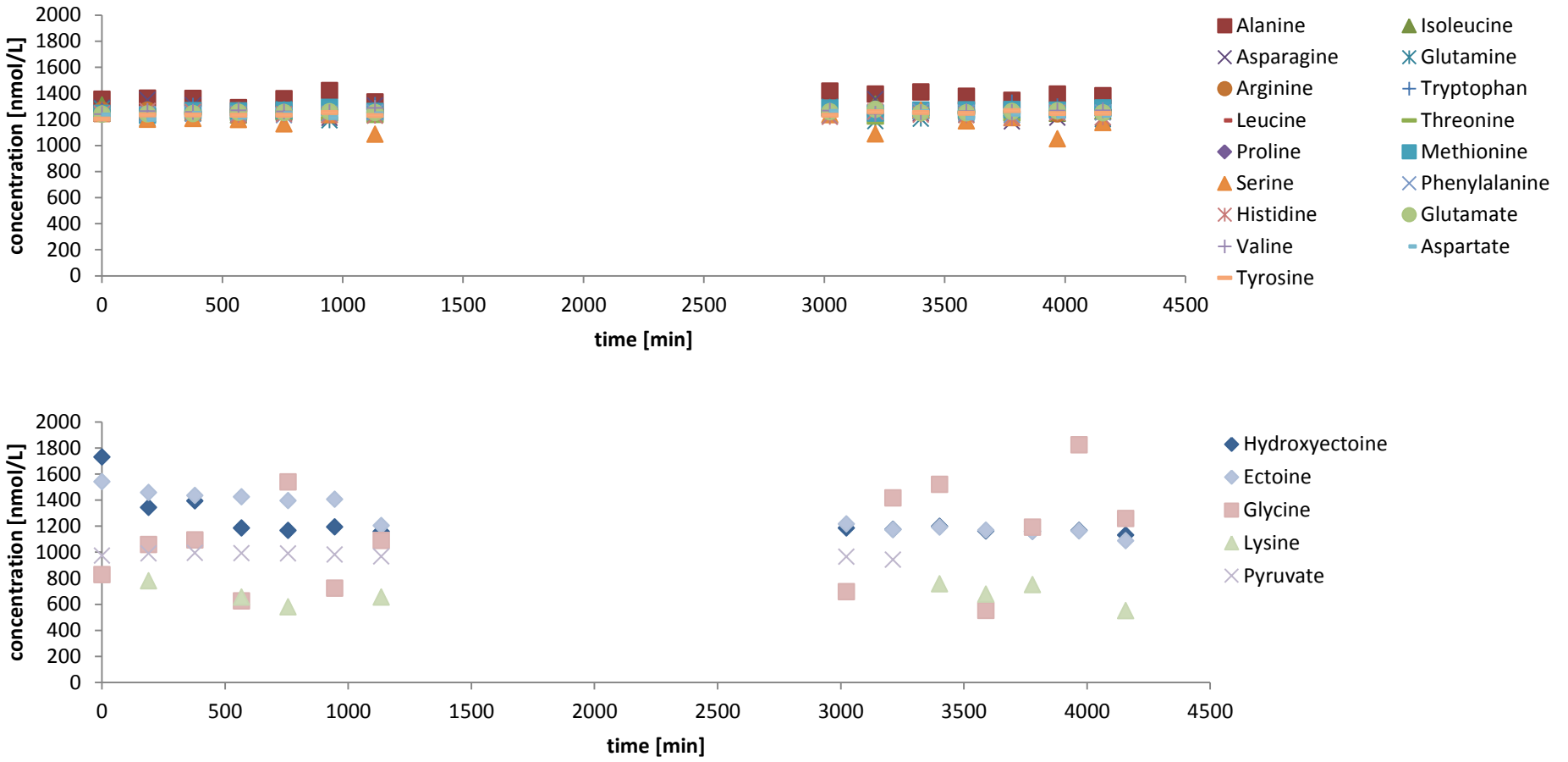

Figure 2 Measured concentrations of targeted analytes in a QC sample over the time of the measurements (negative (Pyr) and positive ion (all analytes but Pyr) mode). Except Pyr (IC-method) all analytes were measured conducting the RP-method. For the RP-method a 1250 nM standard, while for the IC-method a 1000 nM standard was used as QC.

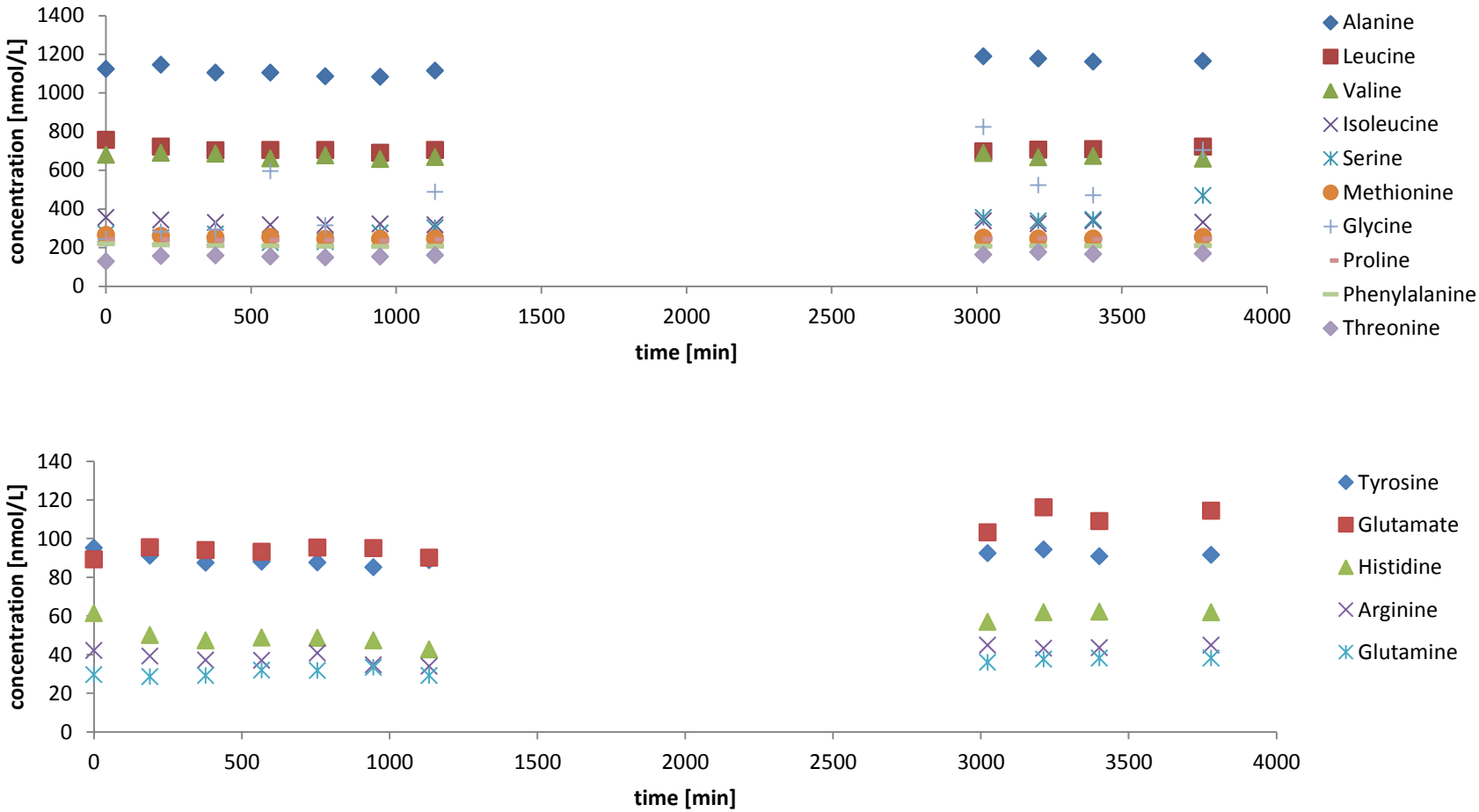

Figure 3 Measured concentrations of targeted analytes in a pooled sample over the time of the RP-measurement.

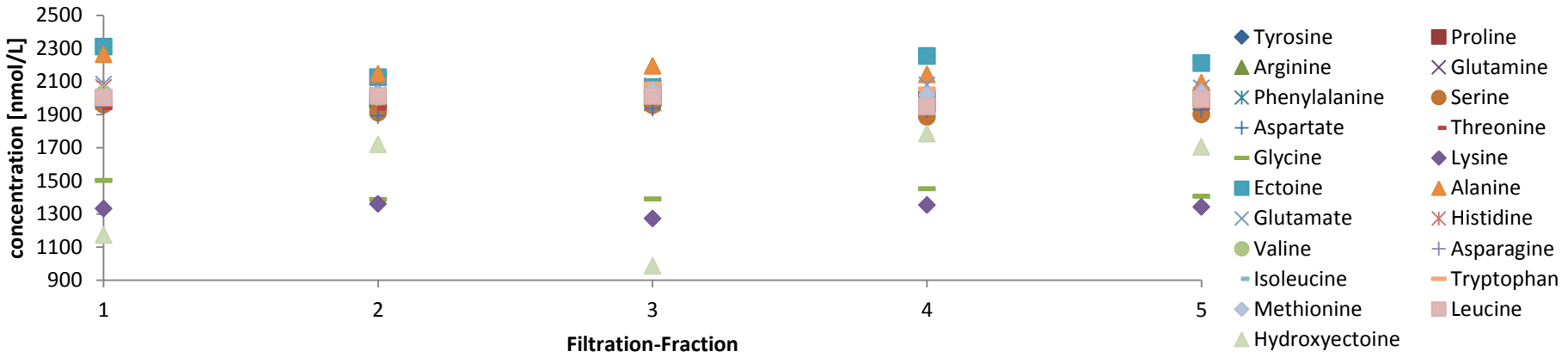

Figure 4 Measured concentrations of different filtration-fractions of a 2000 nM Standard. Filtration-fraction 1 refers to the un-filtrated standard. The other fractions are refereeing to 4 mL pressed through a single filter. Each fraction consisted of 1 mL

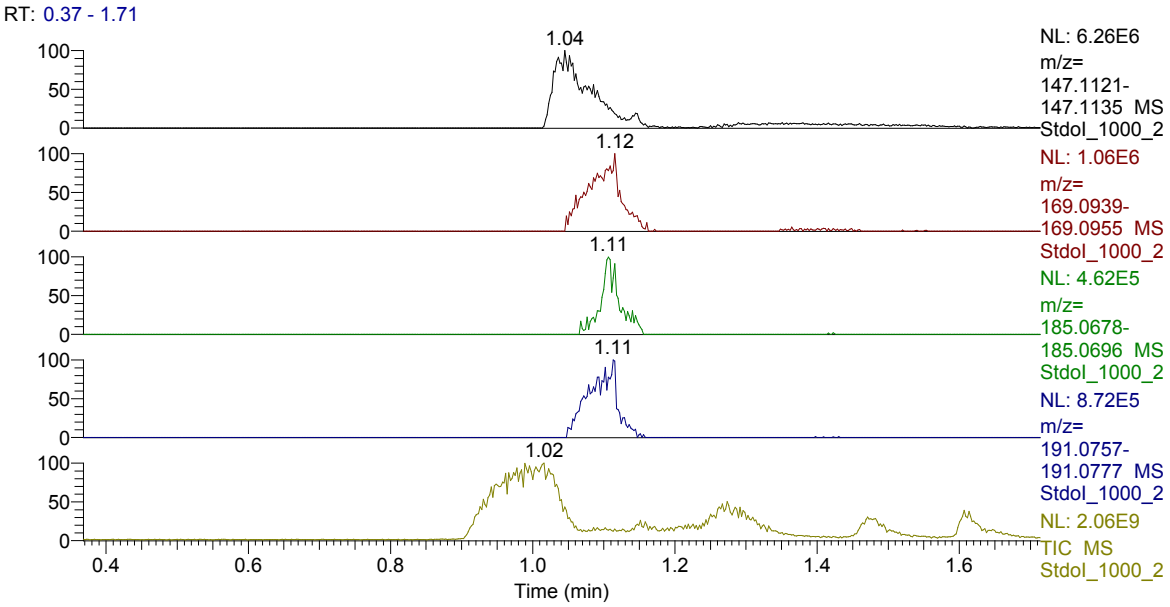

Figure 5 Comparisons of different adduct peaks of lysine and the total ion chromatogram (TIC) in a 10 µM standard. From top to down the different chromatograms are referring to the $[M+H]^+$, $[M+Na]^+$, $[M+K]^+$ and $[M+2Na-H]^+$ adducts of lysine and the TIC at the bottom.

3.1.3 Cell culture results

3.1.3.1 Targeted analysis

The concentrations of the measured samples are given for both time points in **Table 5** and **Table 6** respectively (in **Table 6** corresponding LOQs are given). The normalised monoculture concentrations are given in **Table 7**. Those concentrations were normalised by a measure for the amount of cells present in the culture at the sampling time (**Figure 6**). The cell count was performed by a quantitative polymerase chain reaction technique (qPCR). For the quantification the number of amoA gene copies and soxB gene copys were used for *N. Gargensis* and the betaproteobacterium respectively. Both genes are only present once per cell. Consequently, those obtained gene counts will be referred to as cell counts in the following sections. The gene counts in the BT monocultures were all found to be below 1500 soxB gene copies/mL and were therefore not further investigated. In the dendrogram in **Figure 7** it can be concluded, that the different sample groups were forming well distinguishable clusters, which allowed distinguishing not only between the different cell cultures but also between the different time points. Moreover, the samples BA_T2_3, G_T2_1 and G_T2_5 could be identified as possible outliers. Hence, they were removed from further investigations. One of the main objectives of the present study was to investigate

Table 5 Measured sample concentrations (first time point) of targeted analytes in nmol/L are given for each sample. A heat map was applied for each compound over all biological replicates. Right of the table the legend for the heat map can be seen. Except Pyr (measured employing the IC-method) all metabolites were measured using the RP-method. Pyr was therefore measured in a different technical replicate than the other analytes. Concentrations which were found to be lower than the lowest calibration point (LCP) are not given.

	Concentration [nmol/L]																			
Samples	Ala	Arg	Asn	Asp	Glu	Gln	Gly	His	Ile	Leu	Met	Phe	Pro	Ser	Thr	Trp	Tyr	Val	Pyr	
BA_T1_1	4486	56	323	<LCP	246	<LCP	>10000	100	1059	2913	1131	816	853	1300	648	49	192	2698	419	high
BA_T1_2	3737	44	290	<LCP	471	<LCP	8410	93	943	2366	956	701	668	969	553	37	162	2297	494	
BA_T1_3	4101	43	215	<LCP	961	<LCP	8387	105	1036	2090	943	785	756	873	690	60	203	2080	664	
BA_T1_4	3665	41	260	<LCP	323	<LCP	6755	79	902	2458	850	697	668	908	501	30	137	2470	462	
BA_T1_5	4427	68	385	<LCP	80	<LCP	6419	109	1143	3164	1202	901	924	1321	512	57	214	2953	308	
BM_T1_1	<LCP	<LCP	<LCP	<LCP	<LCP	<LCP	<LCP	<LCP	19	53	<LCP	27	64	<LCP	<LCP	<LCP	<LCP	32	<LCP	
BM_T1_2	<LCP	18	<LCP	<LCP	<LCP	<LCP	<LCP	26	19	34	<LCP	26	68	<LCP	27	<LCP	<LCP	41	<LCP	
BM_T1_3	<LCP	<LCP	<LCP	<LCP	<LCP	<LCP	<LCP	<LCP	<LCP	46	<LCP	29	64	<LCP	<LCP	<LCP	<LCP	35	<LCP	
BM_T1_4	<LCP	<LCP	<LCP	<LCP	24	<LCP	<LCP	<LCP	34	41	<LCP	25	99	<LCP	41	<LCP	<LCP	63	<LCP	
BM_T1_5	<LCP	<LCP	<LCP	<LCP	<LCP	<LCP	<LCP	<LCP	15	45	<LCP	30	70	<LCP	<LCP	<LCP	<LCP	40	<LCP	
BT_T1_1	<LCP	<LCP	<LCP	<LCP	<LCP	<LCP	<LCP	<LCP	<LCP	<LCP	<LCP	<LCP	<LCP	<LCP	36	<LCP	<LCP	<LCP	228	
BT_T1_2	<LCP	<LCP	<LCP	<LCP	<LCP	<LCP	<LCP	<LCP	<LCP	<LCP	<LCP	<LCP	<LCP	<LCP	42	<LCP	<LCP	<LCP	195	
BT_T1_3	<LCP	<LCP	<LCP	<LCP	<LCP	<LCP	<LCP	<LCP	<LCP	<LCP	<LCP	<LCP	<LCP	<LCP	24	<LCP	<LCP	<LCP	196	
BT_T1_4	<LCP	<LCP	<LCP	<LCP	<LCP	<LCP	<LCP	<LCP	<LCP	<LCP	<LCP	<LCP	<LCP	<LCP	45	<LCP	<LCP	<LCP	194	
BT_T1_5	<LCP	<LCP	<LCP	<LCP	<LCP	<LCP	<LCP	<LCP	<LCP	<LCP	<LCP	<LCP	<LCP	<LCP	<LCP	<LCP	<LCP	<LCP	194	
G_T1_1	498	50	<LCP	<LCP	152	109	<LCP	60	211	176	24	98	95	71	117	<LCP	111	200	377	
G_T1_2	534	51	<LCP	<LCP	146	118	<LCP	45	226	189	28	99	90	<LCP	104	<LCP	110	219	378	
G_T1_3	653	57	<LCP	<LCP	163	119	<LCP	48	236	197	35	104	101	<LCP	113	<LCP	116	247	372	
G_T1_4	657	56	<LCP	<LCP	158	120	<LCP	44	240	190	32	100	98	<LCP	115	<LCP	112	234	359	
G_T1_5	637	53	<LCP	<LCP	160	121	<LCP	56	237	192	31	100	97	<LCP	109	<LCP	116	234	366	
BG_T1_1	<LCP	46	<LCP	<LCP	<LCP	<LCP	<LCP	45	174	154	<LCP	86	94	<LCP	<LCP	<LCP	95	107	93	
BG_T1_2	<LCP	51	<LCP	<LCP	<LCP	<LCP	<LCP	43	191	159	<LCP	86	95	<LCP	18	<LCP	97	104	607	
BG_T1_3	<LCP	52	<LCP	<LCP	<LCP	<LCP	<LCP	47	190	181	<LCP	92	100	<LCP	24	<LCP	101	103	126	
BG_T1_4	<LCP	49	<LCP	<LCP	<LCP	<LCP	<LCP	46	188	162	<LCP	85	98	<LCP	<LCP	<LCP	94	98	105	
BG_T1_5	<LCP	46	<LCP	<LCP	<LCP	<LCP	<LCP	39	180	153	19	86	100	<LCP	37	<LCP	96	119	112	low

Table 6 Measured sample concentrations (second time point) of targeted analytes in nmol/L are given for each sample. A heat map was applied for each compound over all biological replicates. Right of the table the legend for the heat map can be seen. Except Pyr (measured employing the IC-method) all metabolites were measured using the RP-method. Pyr was therefore measured in a different technical replicate than the other analytes. All LOQs have been calculated by multiplying the standard deviation of three standards of the same concentration by 10 (according to the Eurachem guide from 2014). The standards used for this were always the lowest concentrated standards for which a peak could be observed and integrated in all replicates. Hence different concentrations were used for different components (a…16 nM, b…31 nM, c…125 nM, d…1250 nM and e…2500 nM). For Pyr no LOQ could be calculated as all standards were injected only once. However, the calculated LOQs do not necessarily reflect the true concentration under which no reliable quantifications is possible anymore. Consequently, also concentrations lower than the LOQs are given in the table if the peak shape looked convincing to the author. Concentrations which were found to be lower than the lowest calibration point (LCP) are not given.

	Concentration [nmol/L]																		
	Ala	Arg	Asn	Asp	Glu	Gln	Gly	His	Ile	Leu	Met	Phe	Pro	Ser	Thr	Trp	Tyr	Val	Pyr
LOQ	11[a]	4[b]	120[c]	343[c]	15[b]	2[b]	2429[d]	161[a]	10[b]	3[a]	10[b]	9[b]	12[b]	632[c]	107[b]	22[b]	9[b]	21[b]	
Samples																			
BA_T2_1	533	143	530	<LCP	118	56	<LCP	180	742	2468	1281	913	779	<LCP	1108	106	366	263	551
BA_T2_2	919	139	472	<LCP	111	36	<LCP	244	805	2640	1436	1074	860	89	1520	134	439	595	546
BA_T2_3	<LCP	152	524	107	439	63	<LCP	304	2699	4484	3093	1886	1978	948	1147	285	697	4114	447
BA_T2_4	391	98	425	<LCP	37	20	<LCP	118	595	2080	918	822	683	<LCP	904	66	251	280	941
BA_T2_5	534	191	473	<LCP	68	53	<LCP	224	642	2150	1190	836	739	409	1141	86	312	428	411
BM_T2_1	<LCP	30	<LCP	<LCP	22	<LCP	<LCP	34	104	239	<LCP	142	223	<LCP	<LCP	35	35	64	660
BM_T2_2	<LCP	19	<LCP	<LCP	21	<LCP	<LCP	31	131	271	25	181	246	<LCP	<LCP	42	44	75	1002
BM_T2_3	<LCP	21	<LCP	<LCP	23	<LCP	<LCP	39	147	324	25	211	279	<LCP	<LCP	51	55	75	831
BM_T2_4	<LCP	<LCP	<LCP	<LCP	<LCP	<LCP	<LCP	31	122	264	25	161	233	<LCP	<LCP	40	38	66	1003
BM_T2_5	<LCP	20	<LCP	<LCP	<LCP	<LCP	<LCP	35	132	305	21	180	252	<LCP	<LCP	45	43	71	676
BT_T2_1	<LCP	<LCP	<LCP	<LCP	<LCP	<LCP	<LCP	<LCP	<LCP	<LCP	<LCP	<LCP	<LCP	<LCP	<LCP	<LCP	<LCP	<LCP	190
BT_T2_2	<LCP	<LCP	<LCP	<LCP	<LCP	<LCP	<LCP	<LCP	<LCP	<LCP	<LCP	<LCP	<LCP	<LCP	<LCP	<LCP	<LCP	<LCP	171
BT_T2_3	<LCP	<LCP	<LCP	<LCP	<LCP	<LCP	<LCP	<LCP	<LCP	<LCP	<LCP	<LCP	<LCP	<LCP	<LCP	<LCP	<LCP	<LCP	76
BT_T2_4	<LCP	<LCP	<LCP	<LCP	<LCP	<LCP	<LCP	<LCP	<LCP	<LCP	<LCP	<LCP	<LCP	<LCP	<LCP	<LCP	<LCP	<LCP	80
BT_T2_5	<LCP	<LCP	<LCP	<LCP	<LCP	<LCP	<LCP	<LCP	<LCP	<LCP	<LCP	<LCP	<LCP	<LCP	<LCP	<LCP	<LCP	<LCP	103
G_T2_1	623	62	<LCP	<LCP	172	139	1138	59	234	193	31	110	107	91	113	<LCP	126	229	444
G_T2_2	657	67	<LCP	<LCP	183	158	<LCP	56	263	219	32	118	116	77	124	<LCP	137	249	413
G_T2_3	803	61	<LCP	<LCP	215	197	<LCP	59	274	216	35	114	115	<LCP	110	<LCP	135	276	488
G_T2_4	789	63	<LCP	<LCP	189	192	<LCP	60	275	147	33	112	115	<LCP	110	<LCP	130	271	418
G_T2_5	915	71	<LCP	<LCP	222	177	<LCP	55	272	221	33	124	134	214	143	<LCP	149	313	528
BG_T2_1	<LCP	60	<LCP	<LCP	<LCP	<LCP	<LCP	59	194	177	16	106	118	<LCP	<LCP	<LCP	117	105	144
BG_T2_2	35	64	<LCP	<LCP	<LCP	<LCP	<LCP	62	209	191	18	109	119	<LCP	35	<LCP	118	122	117
BG_T2_3	<LCP	59	<LCP	<LCP	<LCP	<LCP	<LCP	51	192	184	17	104	116	<LCP	<LCP	<LCP	114	105	109
BG_T2_4	<LCP	68	<LCP	<LCP	<LCP	<LCP	<LCP	52	203	196	<LCP	114	136	<LCP	25	<LCP	121	121	133
BG_T2_5	35	61	<LCP	<LCP	<LCP	<LCP	<LCP	55	218	173	23	106	116	<LCP	44	<LCP	111	155	67

high … low

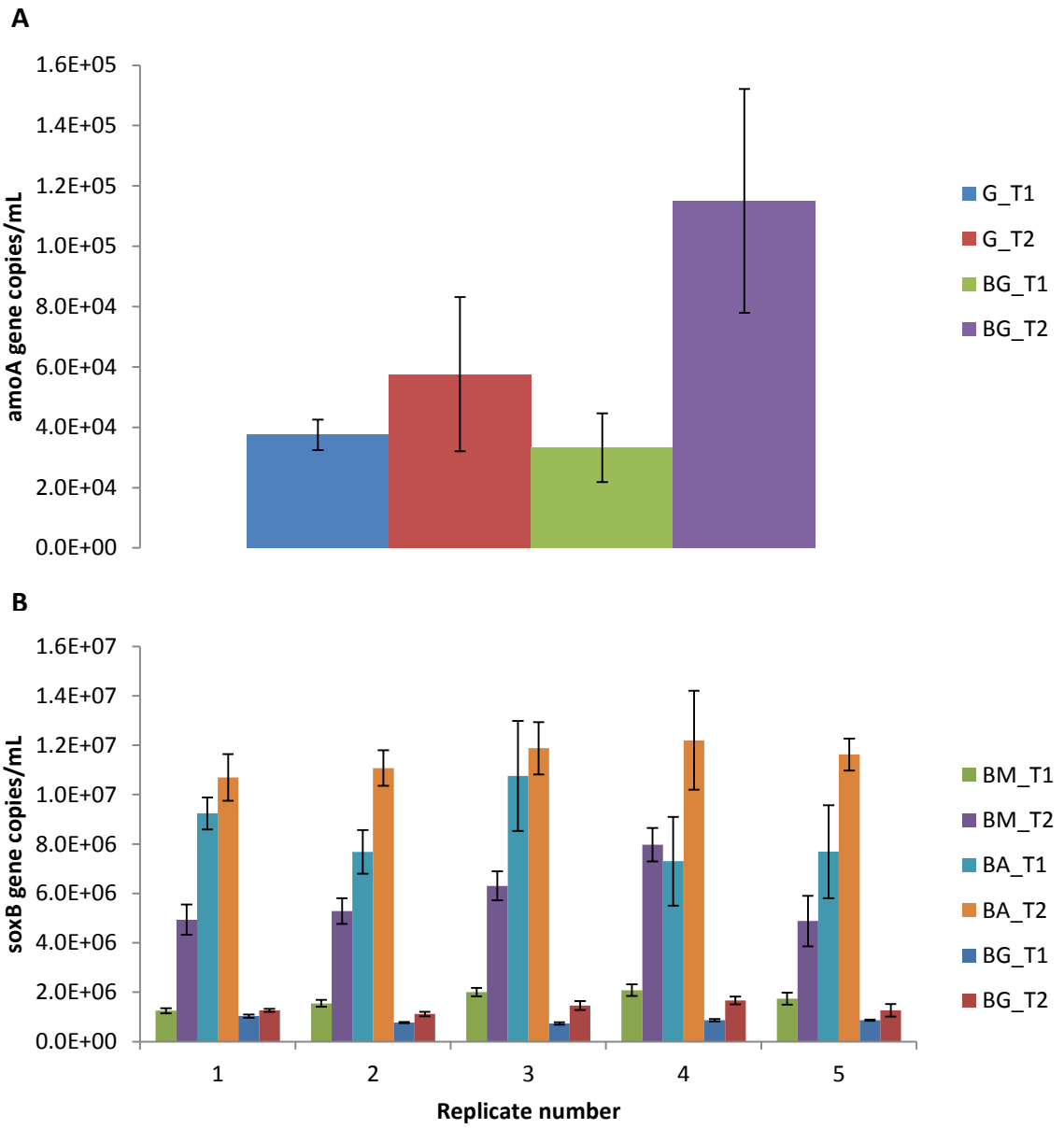

Figure 6 Gene counts (amoA gene copies for *N. Gargensis* (A) and soxB gene copys for the betaproteobacterium (B)) of all considered monocultures (obtained by qPCR) which were used for normalisation purposes are given in this diagram. Except for the *N. Gargensis* monocultures (G_T1_1-5 and G_T2_1-5) each culture was investigated individually. In case of the *N. Gargensis* cultures the average cell count was used for all cultures.

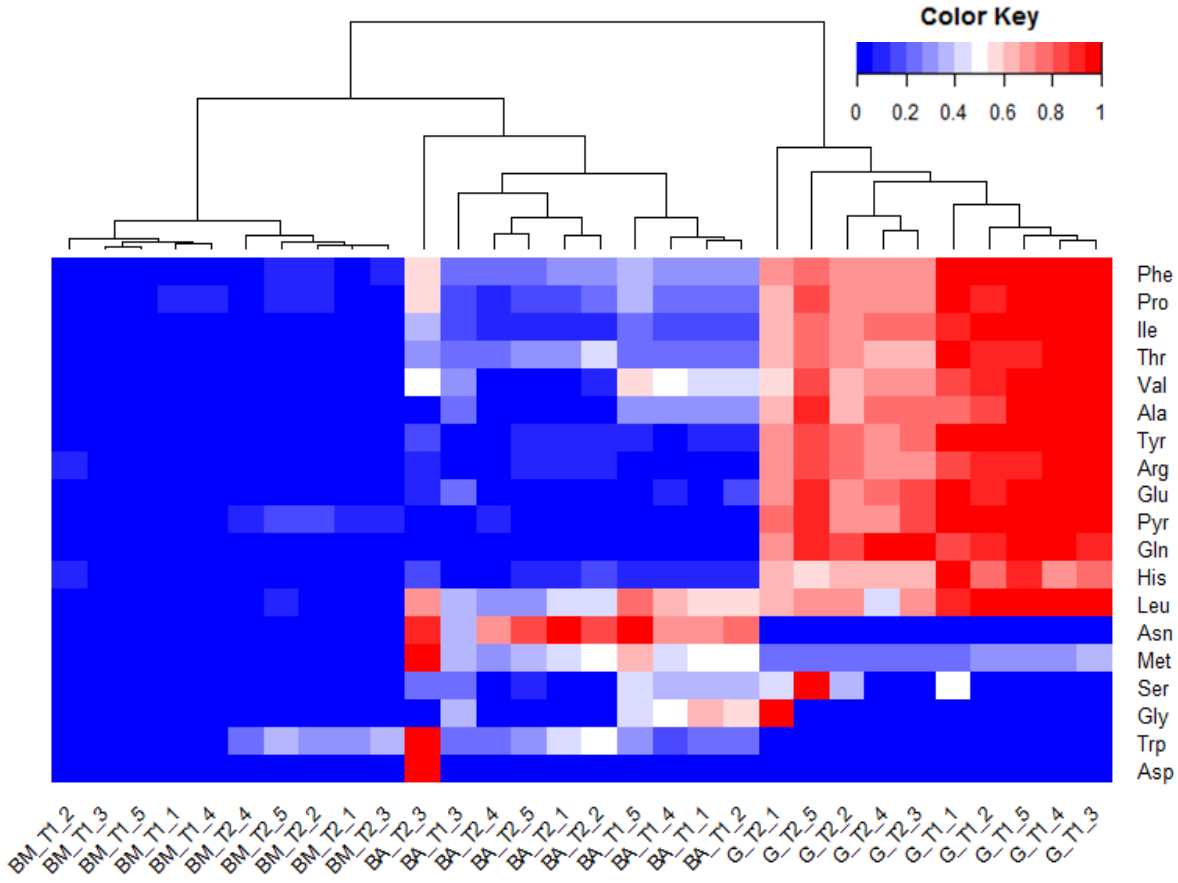

Figure 7 Normalised sample concentrations of targeted analytes have been scaled to values between 0 and 1. From the dendrogram it can be concluded that the sample BA_T2_3 is very likely an outlier. The same could be argued for G_T2_1 and G_T2_5

possible interactions between *N. Gargensis* and the betaproteobacterium. In order to do this the concentrations of all targeted analytes within the co-cultures at the second time point (BG_T2) were put into relation with a predicted concentration (**Figure 8**). The predicted concentrations were derived by simply using the rule of three. For example, if x cells lead to a concentration of a, then y cells lead to a concentration of:

$$b = \frac{y*a}{x}$$ **Equation 3**

The corresponding error bars were calculated by error propagation considering the average standard deviations of the *N. Gargensis* cell counts in the monocultures and the co-cultures and the standard deviation of measured analyte concentrations in the monocultures. Due to the high total uncertainty originating from the high uncertainty from the *N. Gargensis* cell counts, not many analytes being different from their expected concentrations could be found. Before further conclusions are drawn, the total uncertainty should therefore be reduced by minimizing the uncertainty of the applied cell counting techniques.

Table 7 Normalised sample concentrations of targeted analytes in pmol/10^6 cells are given for each sample. A heat map was applied for each compound over all biological replicates. Right of the table the legend for the heat map can be seen. Except Pyr (measured employing the IC-method) all metabolites were measured using the RP-method. Pyr was therefore measured in a different technical replicate than the other analytes. Concentrations which were found to be lower than the lowest calibration point (LCP) are not given.

	Concentration [pmol/10^6 cells]																			
Samples	Ala	Arg	Asn	Asp	Glu	Gln	Gly	His	Ile	Leu	Met	Phe	Pro	Ser	Thr	Trp	Tyr	Val	Pyr	
BA_T1_1	486	6	35	<LCP	27	<LCP	>1083	11	115	315	122	88	92	141	70	5	21	292	45	high
BA_T1_2	487	6	38	<LCP	61	<LCP	1096	12	123	308	125	91	87	126	72	5	21	299	64	
BA_T1_3	381	4	20	<LCP	89	<LCP	780	10	96	194	88	73	70	81	64	6	19	193	62	
BA_T1_4	502	6	36	<LCP	44	<LCP	925	11	124	337	116	96	91	124	69	4	19	338	63	
BA_T1_5	576	9	50	<LCP	10	<LCP	835	14	149	412	156	117	120	172	67	7	28	384	40	
BM_T1_1	<LCP	<LCP	<LCP	<LCP	<LCP	<LCP	<LCP	<LCP	15	42	<LCP	22	51	<LCP	<LCP	<LCP	<LCP	25	<LCP	
BM_T1_2	<LCP	12	<LCP	<LCP	<LCP	<LCP	<LCP	17	13	22	<LCP	17	44	<LCP	17	<LCP	<LCP	26	<LCP	
BM_T1_3	<LCP	<LCP	<LCP	<LCP	<LCP	<LCP	<LCP	<LCP	<LCP	23	<LCP	15	32	<LCP	<LCP	<LCP	<LCP	17	<LCP	
BM_T1_4	<LCP	<LCP	<LCP	<LCP	11	<LCP	<LCP	<LCP	16	20	<LCP	12	48	<LCP	20	<LCP	<LCP	30	<LCP	
BM_T1_5	<LCP	<LCP	<LCP	<LCP	<LCP	<LCP	<LCP	<LCP	9	26	<LCP	18	40	<LCP	<LCP	<LCP	<LCP	23	<LCP	
G_T1_1	13279	1325	<LCP	<LCP	4055	2909	<LCP	1596	5622	4695	632	2618	2546	1893	3128	<LCP	2952	5336	10058	
G_T1_2	14227	1350	<LCP	<LCP	3896	3145	<LCP	1191	6014	5047	741	2651	2393	<LCP	2784	<LCP	2923	5837	10074	
G_T1_3	17401	1532	<LCP	<LCP	4341	3174	<LCP	1274	6283	5247	936	2780	2699	<LCP	3013	<LCP	3105	6577	9907	
G_T1_4	17531	1484	<LCP	<LCP	4208	3209	<LCP	1169	6397	5054	854	2657	2618	<LCP	3059	<LCP	2989	6237	9564	
G_T1_5	16986	1423	<LCP	<LCP	4273	3236	<LCP	1483	6330	5115	831	2679	2598	<LCP	2912	<LCP	3097	6242	9757	
BA_T2_1	50	13	50	<LCP	11	5	<LCP	17	69	231	120	85	73	<LCP	104	10	34	25	52	
BA_T2_2	83	13	43	<LCP	10	3	<LCP	22	73	238	130	97	78	8	137	12	40	54	49	
BA_T2_3	<LCP	13	44	9	37	5	<LCP	26	227	378	260	159	167	80	97	24	59	346	38	
BA_T2_4	32	8	35	<LCP	3	2	<LCP	10	49	171	75	67	56	<LCP	74	5	21	23	77	
BA_T2_5	46	16	41	<LCP	6	5	<LCP	19	55	185	102	72	64	35	98	7	27	37	35	
BM_T2_1	<LCP	6	<LCP	<LCP	4	<LCP	<LCP	7	21	48	<LCP	29	45	<LCP	<LCP	7	7	13	134	
BM_T2_2	<LCP	4	<LCP	<LCP	4	<LCP	<LCP	6	25	51	5	34	47	<LCP	<LCP	8	8	14	190	
BM_T2_3	<LCP	3	<LCP	<LCP	4	<LCP	<LCP	6	23	51	4	33	44	<LCP	<LCP	8	9	12	132	
BM_T2_4	<LCP	<LCP	<LCP	<LCP	<LCP	<LCP	<LCP	4	15	33	3	20	29	<LCP	<LCP	5	5	8	126	
BM_T2_5	<LCP	4	<LCP	<LCP	<LCP	<LCP	<LCP	7	27	62	4	37	52	<LCP	<LCP	9	9	15	139	
G_T2_1	10816	1076	<LCP	<LCP	2986	2413	19757	1024	4063	3351	538	1910	1858	1580	1962	<LCP	2188	3976	7705	
G_T2_2	11406	1163	<LCP	<LCP	3177	2743	<LCP	972	4566	3802	556	2049	2014	1337	2153	<LCP	2378	4323	7177	
G_T2_3	13941	1059	<LCP	<LCP	3733	3420	<LCP	1024	4757	3750	608	1979	1997	<LCP	1910	<LCP	2344	4792	8474	
G_T2_4	13698	1094	<LCP	<LCP	3281	3333	<LCP	1042	4774	2552	573	1944	1997	<LCP	1910	<LCP	2257	4705	7265	
G_T2_5	15885	1233	<LCP	<LCP	3854	3073	<LCP	955	4722	3837	573	2153	2326	3715	2483	<LCP	2587	5434	9174	low

3.1.3.2 Untargeted analysis

An overview over the data obtained by untargeted data evaluation is given in the heat maps in **Figure 9** and **Figure 10** for RP and IC data respectively. All of them show that good clustering could be obtained for all different sample groups. The only exception was BA_T2_4 which was put in the cluster of the BA_T1 sample group, as can be seen when looking into the IC-heat map. For untargeted data the observed intensities of the different monocultures were not compared with predicted intensities of the co-cultures as performed for the targeted data in **Figure 8** as there were too many influencing factors to draw any conclusions from such a comparison. Features that were annotated with compound names by CD utilising MS2 spectra comparison with mzCloud are given in **Table 8**. Technically they should count as level 2 identifications as described in the introduction. However, the process of spectra comparison could not be fully investigated within the frame of this master thesis project. Hence, given annotation should only be taken as first hints. The data obtained from the co-cultures cannot be compared with the other cultures as it was done and shown for the monoculture data. This is due to the fact that it makes no sense to normalise for the combined cell count of both organisms. However, it can be argued that it makes sense to normalise for only one of the two organisms and thereby check if the other organism had an influence at all. As there was no significant difference between the *N. gargensis* cell counts of BG_T1 and G_T1 it was not necessary to normalise them in order to compare them. In **Figure 11** it can be seen that it was clearly possible to find compounds that show significant differences in concentration when also the betaproteobacterium was present in the culture. Another issue that had to be excluded was the possibility that the investigated organisms leaked into their supernatant due to any sample preparation steps. Therefore samples of the cells which were frozen prior to filtration, in order to lyse them, were compared to the unfrozen replicates in **Figure 12**. It is easily visible that the purposely lysed cells could not be clearly distinguished from those only filtrated. Hence, it was not possible to exclude the possibility that the investigated cells lysed during sample preparation and further investigations on this issue have to be made in the future.

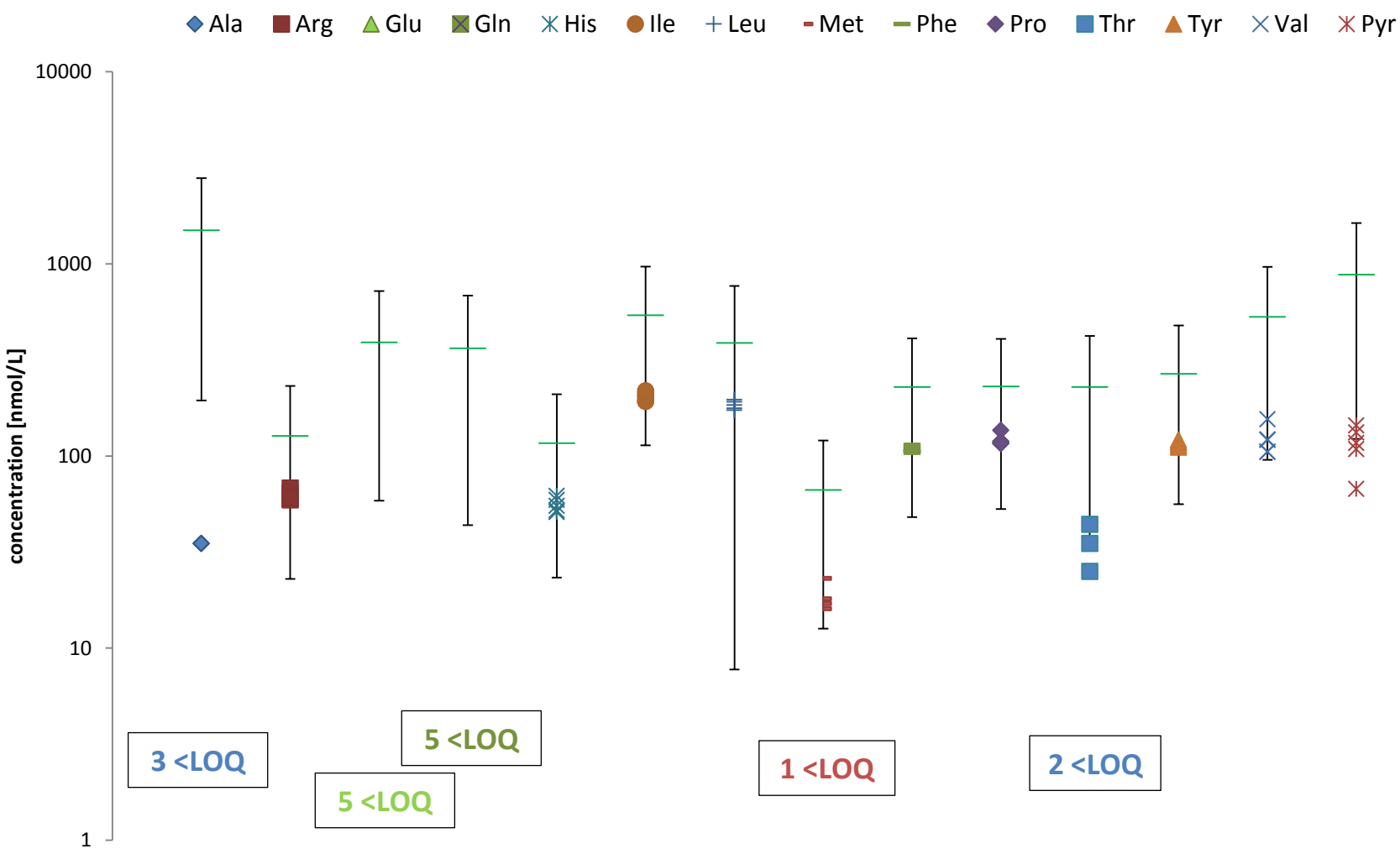

Figure 8 Concentrations measured in different co-cultures are given for all targeted analytes that have been found in at least 2 replicates. The number of replicates below the LOQ is given in black boxes for each analyte. The green lines indicate the expected concentrations, which were derived by comparing the amounts of *N. Gargensis* cells in the monocultures and the co-culture (**Equation 3**). Shown error bars were calculated by error propagation considering the average standard deviations of the *N. Gargensis* cell counts in the monocultures and the co-cultures and the standard deviation of measured analyte concentrations in the monocultures.

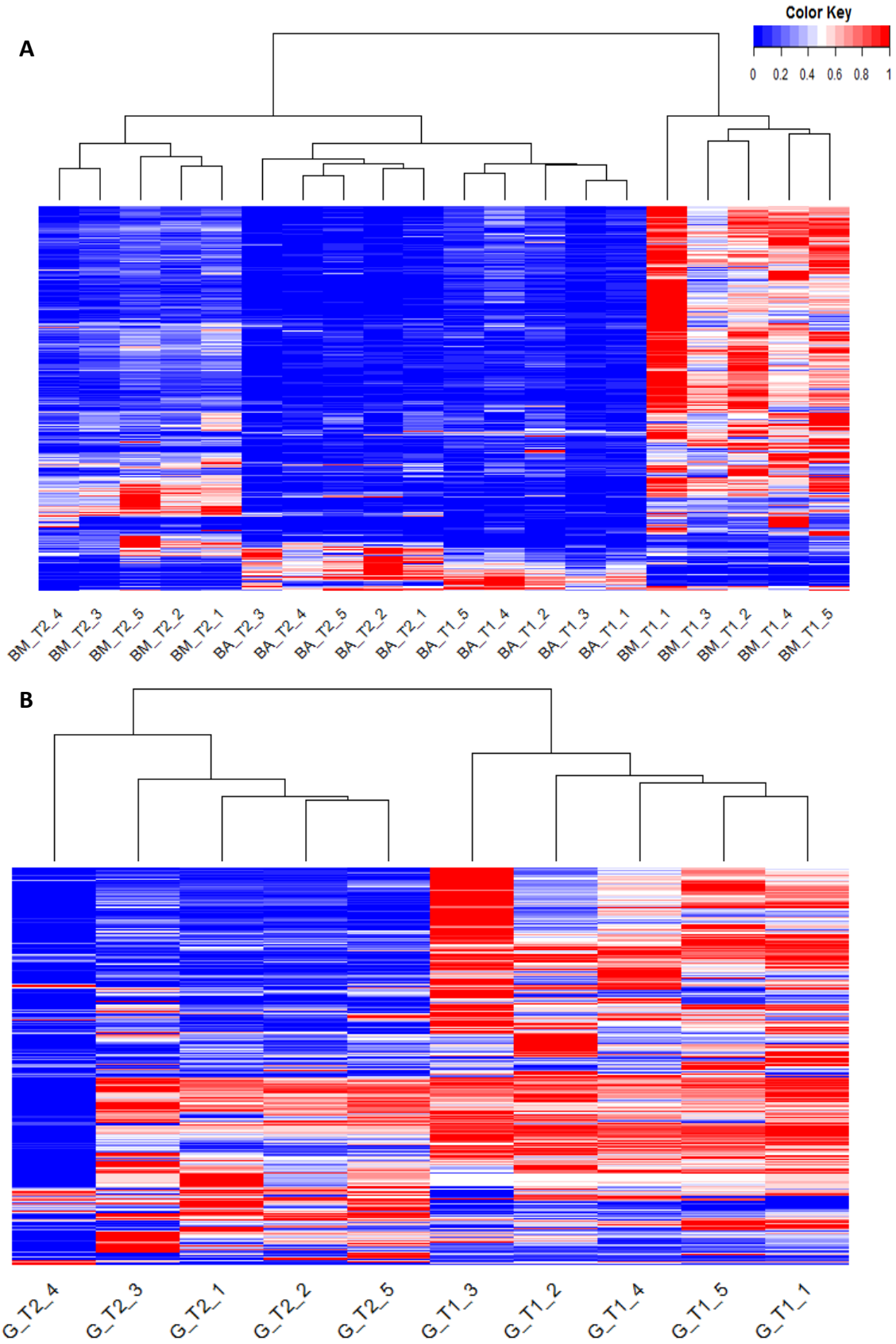

Figure 9 In this overview over untargeted data obtained from RP-MS analysis only the 1715 features that were at least 3 times more intense then the corresponding features in the blanks and had an peak area of at least 1E4 signal intensity*s^{-1} in all replicates of at least one sample group with a FV% of less than 50% were considered. All areas have been normalised for the cell counts of the related cultures and were then scaled to values between 0 and 1. Due to very normalised high signal intensity differences between the sample groups G_T1 and G_T2 and the other sample groups they were separated into different heat maps with G_T1 and G_T2 in heat map B and the others in heat map A.

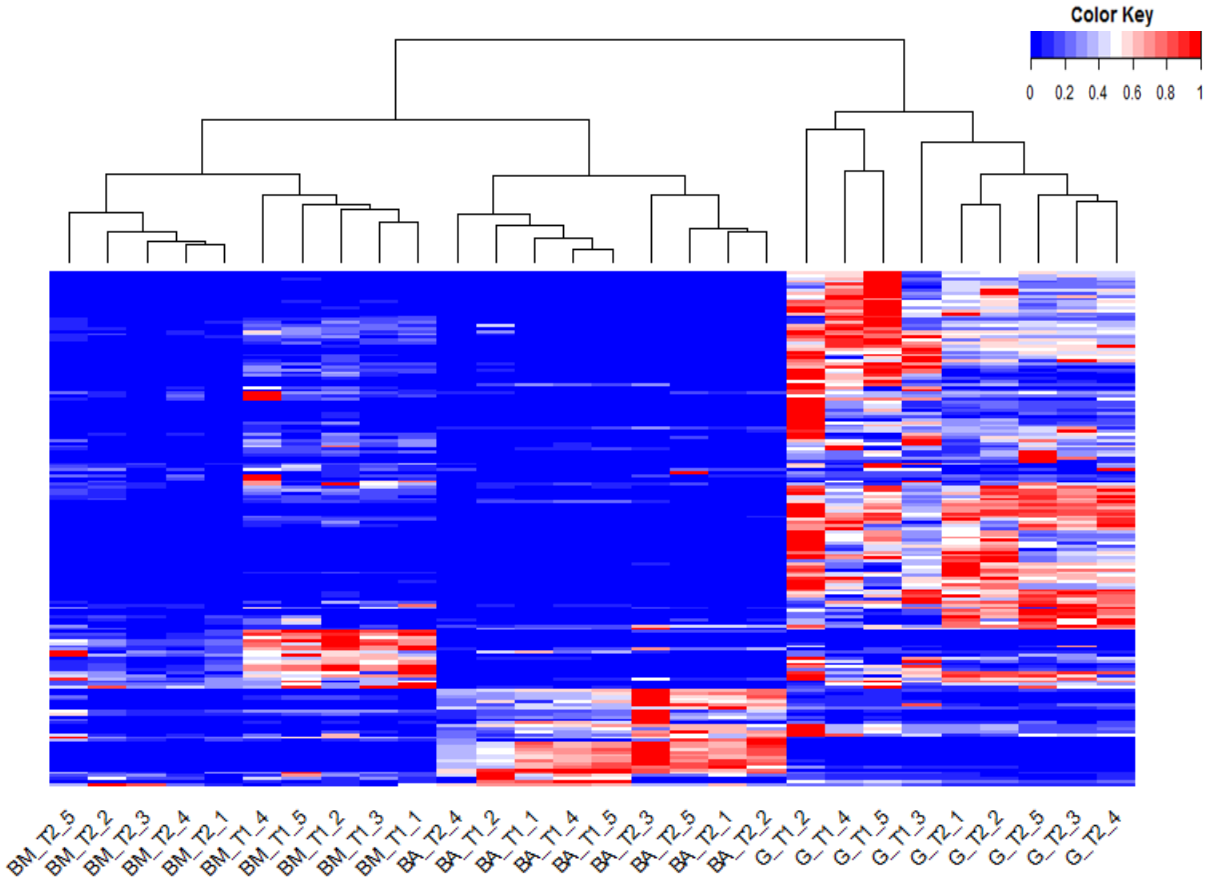

Figure 10 In this overview over untargeted data obtained from IC-MS analysis only the 148 features that were at least 3 times more intense then the corresponding features in the blanks and had an peak area of at least 1E4 signal intensity*s^{-1} in all replicates of at least one sample group with a FV% of less than 50% were considered. All areas have been normalised for the cell counts of the related cultures and were then scaled to values between 0 and 1. As G_T1_1 and BA_T1_3 have not been measured with the IC-method they are not shown here.

Table 8 In this overview over annotated compounds within the untargeted data obtained by RP-MS and IC-MS analysis only features that were at least 3 times more intense then the corresponding features in the blanks and had an peak area of at least 1E4 signal intensity*s^{-1} in all replicates of at least one sample group with a FV% of less than 50% were considered. For the IC-method this was true for 148 and for the RP-method for 1715 features.

Annotated compounds using the RP-method	
(-)-Camphor	Guanine
1,2,3,4-Tetramethyl-1,3-cyclopentadiene	L-(-)-Methionine
12-Aminododecanoic acid	L-(+)-Citrulline
2,2,6,6-Tetramethyl-1-piperidinol (TEMPO)	L-Norleucine
2'-Deoxyadenosine	L-Phenylalanine
2'-Deoxyguanosine	L-Tyrosine
3-Hydroxybutyric acid	Melamine
4-Hydroxy-6-methyl-2-pyrone	N,N-Diisopropylethylamine (DIPEA)
4-Hydroxybutyric acid (GHB)	N,N-Dimethylaniline
4-Pyridineacetic acid	N4-Acetyl sulfamethazine
5-Aminolevulinic acid	N-Acetyl-DL-serine
5'-S-Methyl-5'-thioadenosine	Nicotinamide
7-Methylguanine	Nicotinic acid
Adenine	Nootkatone
Adenosine	N-Vinyl-2-pyrrolidone
Caprolactam	Oleamide
Citroflex A-4	Pantothenic acid
Coniine	PEG n5
Cytidine	PEG n6
Cytosine	Polygodial
Decanamide	PPG n4
Dibutyl phosphate	Proline
Diethanolamine	Pyridoxal
Diethyl phthalate	Thymidine
Diethyleneglycol diacetate	Tributyl phosphate
Dihexyl phthalate	Triethylene glycol monobutyl ether
DL-Tryptophan	Uracil
D-Serine	Valine
Erucamide	
Annotated compounds using the IC-method	
4-Acetamidobutanoic acid	N-Acetylaspartic acid
4-Hydroxybutyric acid (GHB)	N-Acetyl-DL-glutamic acid
4-Oxoproline	N-Acetyl-DL-serine
4-Phenolsulfonic acid	Pyruvic acid
Glycolic acid	Salicylic acid
Isobutyric acid	Succinic acid
L-(+)-Lactic acid	

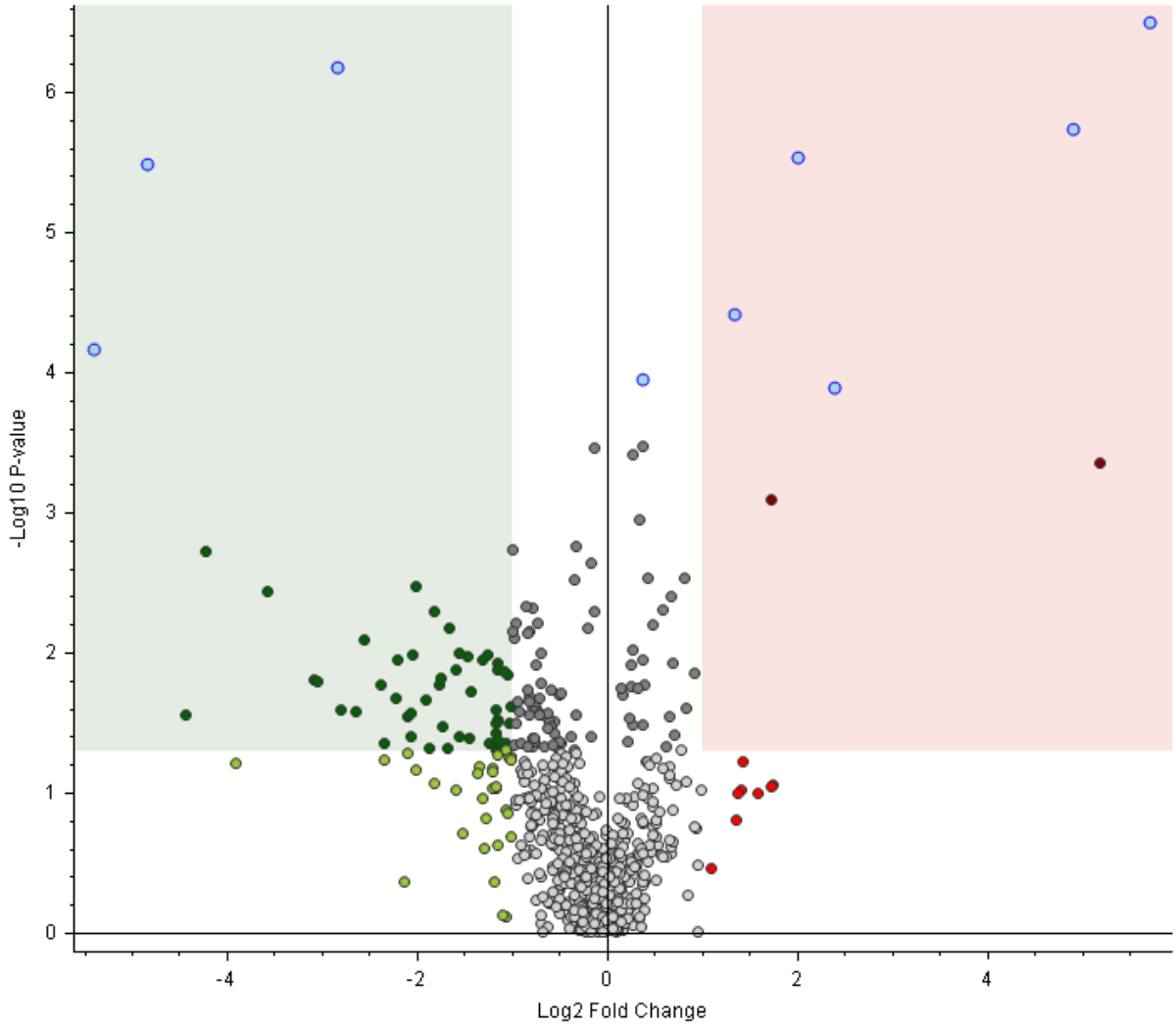

Figure 11 Comparison between BG_T1 and G_T1 via volcano plot. Due to the similar *N. gargensis* cell counts in both sample groups no normalisation was applied. The green area marks the area with a log2 fold change greater than 1 and a p-value below 0.05 with G_T1 having the higher intensity. The red area applies to the case when BG_T1 has the higher intensity. The blue dots indicate those features staying significant after multiple testing correction after Benjamini Hochberg. 7 features are within the red and 52 features within the green box.

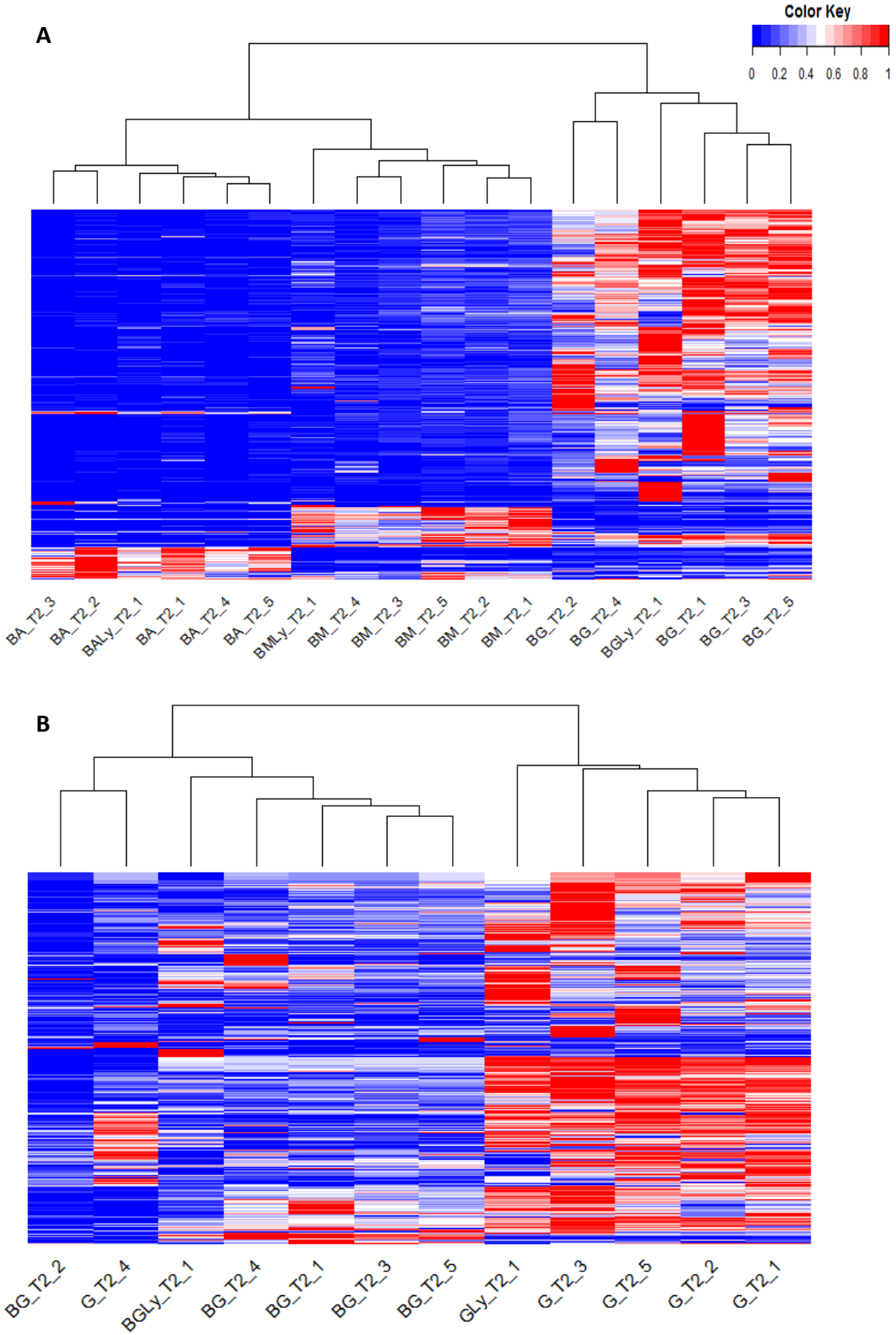

Figure 12 In this overview over untargeted data obtained from RP-MS analysis only the 1715 features that were at least 3 times more intense then the corresponding features in the blanks and had an peak area of at least 1E4 signal intensity*s^{-1} in all replicates of at least one sample group with a FV% of less than 50% were considered. All areas have been normalised for the cell counts of the related cultures (betaproteobacterium in A and N. gargensis in B) and were then scaled to values between 0 and 1. It can be seen that the replicates which were lysed on purpose (BGLy_T2 and GLy_T2) could not be distinguished from other replicates.

3.2 Contamination experiments

The author is aware of the fact that the power of the chosen study set up is quite low due to the low number of procedural replicates. Additionally, the comparisons conducted within the examined contaminant study are kind of arbitrary. This is due to the fact that sample groups (vials, gloves,..) were chosen only from lab materials commonly used at the university, at the time when the study took place. However, the presented study is giving an outline for a possible way to compare lab-equipment regarding to the contaminants they might introduce to samples.

3.2.1 Vials

Utilising the untargeted approach, 911 features were detected within all vial-samples. In order to get rid of unreliable features different filters were applied. With the intention of getting a good overview over the acquired data, a principal component analysis (PCA) was performed (**Figure 13**). For the PCA only features that possessed a peak area higher than 1E4 intensity counts*s^{-1} and FV% below 50% in any of the investigated vial groups from different vendors (MN, TC, H, TN35 and TN41) were taken into account. The resulting PCA scores plot showed good separation of some sample groups and allowed to assess the different sample groups in terms of similarity. It can be seen that the vials from the groups TN35, TN41, H and TC and MN respectively formed easily distinguishable clusters. Sample groups sharing one cluster can therefore be considered to be quite similar. For the assessment of the number of significant compounds within the individual vial groups again only features that exceeded an intensity area threshold of 1E4 intensity count*s^{-1} and a FV% of less than 50% in each sample of at least one sample group were taken into account. An overview of the number of compounds within the different groups is given in the Venn diagram in **Figure 14**. However, the used software (CD) showed peak alignment-problems between different samples, which lead to the problem that in some cases peaks were listed as two different compounds when appearing in more than one sample. Moreover, single peaks were sometimes integrated twice or even more often and therefore count more than once. To overcome those problems listed compounds were counted as one single compound if they had the same accurate mass (± 6 ppm) and RT (± 0.3 min). From the resulting diagram we can conclude that about 124 compounds could be observed in all groups. Therefore, those contaminants might have been present in all investigated vials or they were not related to the vials at all. As the task was to investigate the differences between the vial groups, these compounds were not further

investigated. In **Table 9** always two vial groups are compared regarding the portion of compounds they have in common after subtraction of the 124 compounds present in all groups. The similarities already observed in the PCA are also partly reflected in that table. However, the fact that the differences cannot be observed to the same extent in the table is that PCAs are naturally also taking variations in concentrations into account which are completely neglected in the comparison made in the table and the Venn diagram. It is surprising that only 53% of the compounds were found in TN35 and TN41 as differences between those two groups lied only in the fact that the vials were from a different packages and different caps were used (not sliced and sliced respectively, as described above). Therefore, it cannot be concluded whether the difference is due to the different packages or the different caps from the present data. The closer proximity between TN41 and H compared to TN35 and H in the PCA is also clearly visible in the Venn diagram when the according overlapping regions are considered (59% and 41% respectively). Additionally, it can be easily concluded from the pair-wise comparisons in **Table 9**. The same is true for the

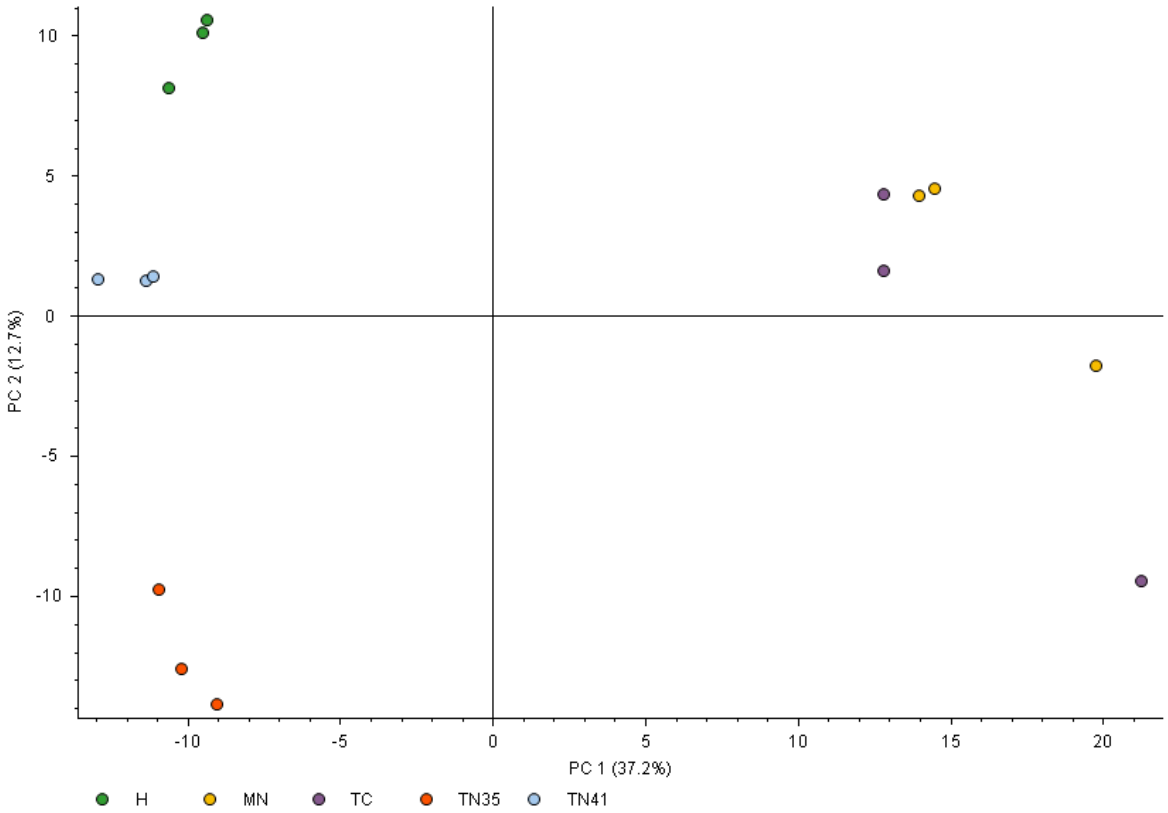

Figure 13 For the shown PCA scores plot only components that were present with an peak area of at least 1E4 signal intensity*s^{-1} in all replicates of at least one vial group vendors with a compound coefficient of variance of less than 50% were considered. The different vial groups contain vials from different vendors.

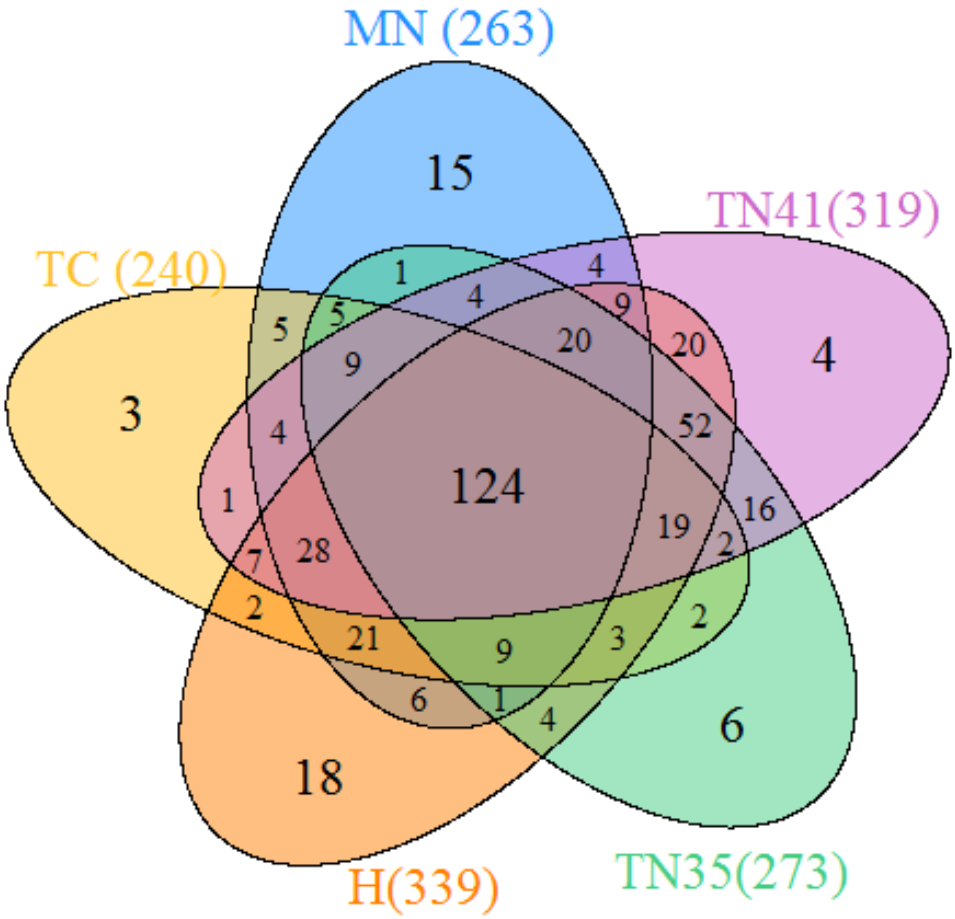

Figure 14 Venn diagram showing the number of compounds within the different vial groups. Only features that exceeded an intensity area threshold of 1E4 intensity count*s^{-1} in each replicate and a FV% of less than 50% were taken into account. The total number of compounds per vial group is given in brackets next to the category labels.

Table 9 Tabulated fractions of components [%] the different vial groups had in common after subtraction of the 53 compounds present in all samples.

	MN [%]	TC [%]	H [%]	TN35 [%]	TN41 [%]
MN [%]	100				
TC [%]	45	100			
H [%]	35	36	100		
TN35 [%]	20	22	41	100	
TN41 [%]	30	28	59	53	100

similarities between MN and TC. However, as already mentioned a more comprehensive data comparison between the different sample groups should not only take into account the mere presence of substances, but also differences in concentrations. Features with signal intensities greater than 1E4 intensity counts*s^{-1}, that showed significant differences

between the sample groups (according to a univariate ANOVA with a subsequent Tukey's range test) are shown in the heat map together with the according dendrogram in **Figure 15**. Various conclusions derived from the PCA in **Figure 13** could be confirmed with the heat map and the according dendrogram. Among those are the facts that TC and MN could not be clearly distinguished. Moreover, the observation that TN41 is more similar to H than H is to TN35 could also be concluded again. As only features that showed an intensity higher than 1E4 counts*s^{-1} were considered it can be concluded that the difference responsible for clustering within the PCA is due to differences in concentration of compounds above the LOD (which was somehow arbitrarily defined at a signal intensity of 1E4 counts*s^{-1}).

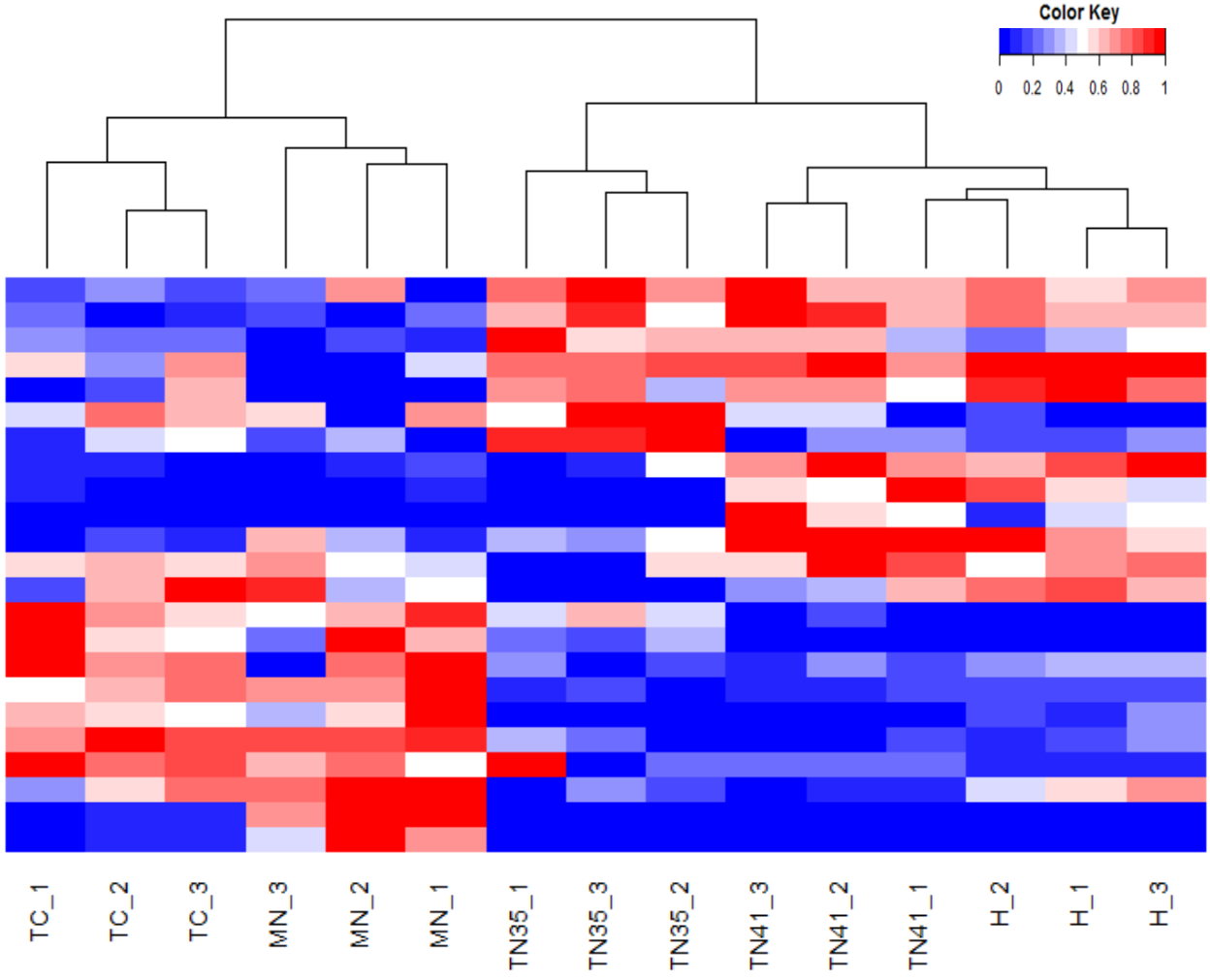

Figure 15 All 110 features (with signal intensities greater than 1E4) showing significant differences ($p_{adj} < 0.05$) between the vial-groups (according to a univariate ANOVA with a subsequent Tukey's range test) were compared sample wise within this heat map. Therefore the concentration range of each individual feature has been scaled to values between 0 and 1.

3.2.1.1 Washed vials

In order to find out if there are possible ways to get rid of vial-associated contaminants, the effect of vial-washing was investigated. Therefore vials from MN were washed either three

times with water or three times with water and three times with methanol and three times with water. In the heat map in **Figure 16** it can be seen that there was a clear effect of washing. The features at the top of the heat map showed a clear tendency of being decreased due to washing while those on the bottom showed the opposite effect. However, possible reasons were not further investigated. A possible explanation for those showing a reverse effect could be decreased ion suppression due to the compounds washed out. However, no obvious difference could be found between those vials washed with methanol and water and those only washed with water.

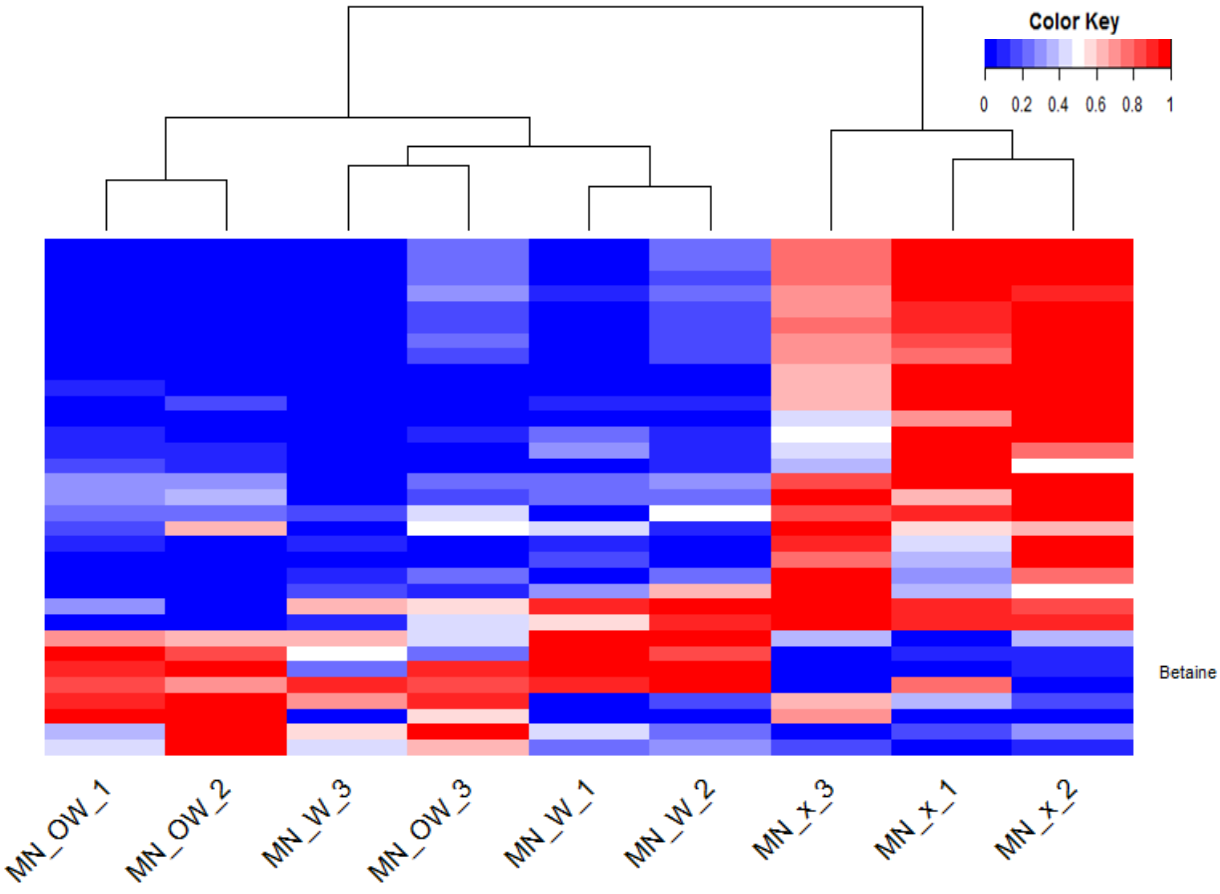

Figure 16 All 33 features (with signal intensities greater than 1E4 counts*s^{-1} and a FV% of less than 50%) showing significant differences (p_{adj} < 0.05) between the differently prepared vial-groups (MN_OW_1-3 with methanol and water, MN_W_1-3 with water and MN_x_1-3 unwashed) (according to a univariate ANOVA with a subsequent Tukey's range test) were compared sample wise within this heat map. Therefore the concentration range of each individual feature has been scaled to values between 0 and 1.

3.2.1.2 Vial caps

The influence of vial caps was investigated for sliced and non-sliced caps. Moreover, the effect of shaking was examined in dependence on the different caps. An overview over the features that showed significant differences between the different sample groups is shown in **Figure 17**. As can be seen, only poor clustering could be achieved for the different sample

groups. However, some clusters could be distinguished. The most striking observation is the big discrepancy between the two unshaken sample groups S_MN and Ss_MN as it implicates that the caps were having an influence on the sample even without direct contact between cap and liquid sample. A possible explanation for this phenomenon is that the needle of the LC system was somehow scrapping contaminants from the caps and subsequently introduced them into the sample. Another cluster contained the sample group with sliced

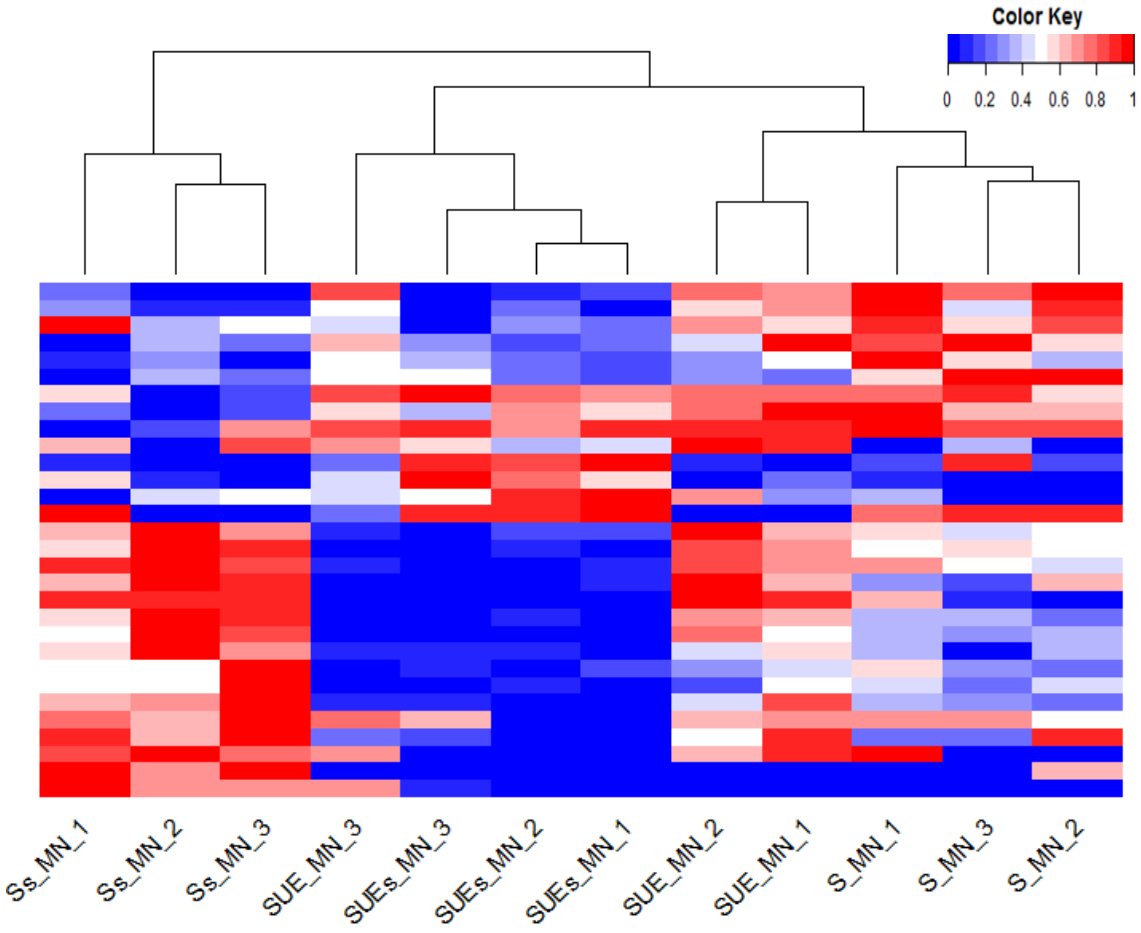

Figure 17 All 30 features (with signal intensities greater than 1E4 counts*s^{-1} and a FV% of less than 50%) showing significant differences ($p_{adj} < 0.05$) between the differently prepared vial cap-groups (Ss_MN_1-3 with sliced caps, SUEs_MN_1-3 with sliced caps and shaken, S_MN_1-3 with unsliced caps and SUE_MN_1-3 with unsliced caps and shaken) (according to a univariate ANOVA with a subsequent Tukey's range test) were compared sample wise within this heat map. Therefore the concentration range of each individual feature has been scaled to values between 0 and 1.

caps that were also shaken (SUEs_MN). The pattern of this cluster is approximately reversed to that of the cluster with sliced caps without shaking (Ss_MN). This could be explained if contaminants, which were introduced by shaking, suppressed the ion formation of those contaminants that were already in the sample.

3.2.2 Gloves

Four different gloves were tested for their leachable small organic substances utilizing an untargeted approach. As for the vial comparisons different filters have been applied for different diagrams in order to get rid of unreliable features as explained in the methods section. Of the four different gloves three were made of nitrile (N) as basic material, while one was composed of latex (L). In the PCA (**Figure 18**) it can be seen that the sample groups KS and SL were very similar to the blank-samples, while the other two groups (BX and SS) are clearly separated. Hence, the glove-sample groups similar to the blank seem to have introduced the least contamination. From the Venn diagram in **Figure 19** it can also be concluded that N gloves from KS and SL showed the least amount of different leachables while SS lead to about 50% more different features (a lot of them unique). The L gloves from BX showed by far the highest amount of unique features. However, it is not only the mere amount of substances that plays a role but also the type of the present substances. Compounds identified via MS2-spectra comparison are given in **Table 10**. When a study is planned it should be considered which compounds could be found as contaminations due to their presence in the used lab materials. In some cases it would surely be advisable to go without specific materials if they could potentially contaminate samples with targeted analytes. In many biological studies it would consequently not make sense to work with latex (a biological product) gloves as they could potential leak biologically relevant substances like valine. In order to investigate significant differences between the sample groups an ANOVA with a subsequent Tukey range test had been performed leading to a number of 52 significantly different compounds ($p < 0.05$). An overview of the different compounds is given in the heat map in **Figure 20**. As only significantly different components were used, the clustering of the different sample groups works naturally better than in the shown PCA where no such measure for significance was taken into account. However, similar conclusions as already discussed for the PCA can still be drawn. Overall, it can be said that regarding the leaching of small molecules from the gloves from the sample groups SS and BX (or latex in general) should be used with caution as a lot of different contaminants could potentially be introduced.

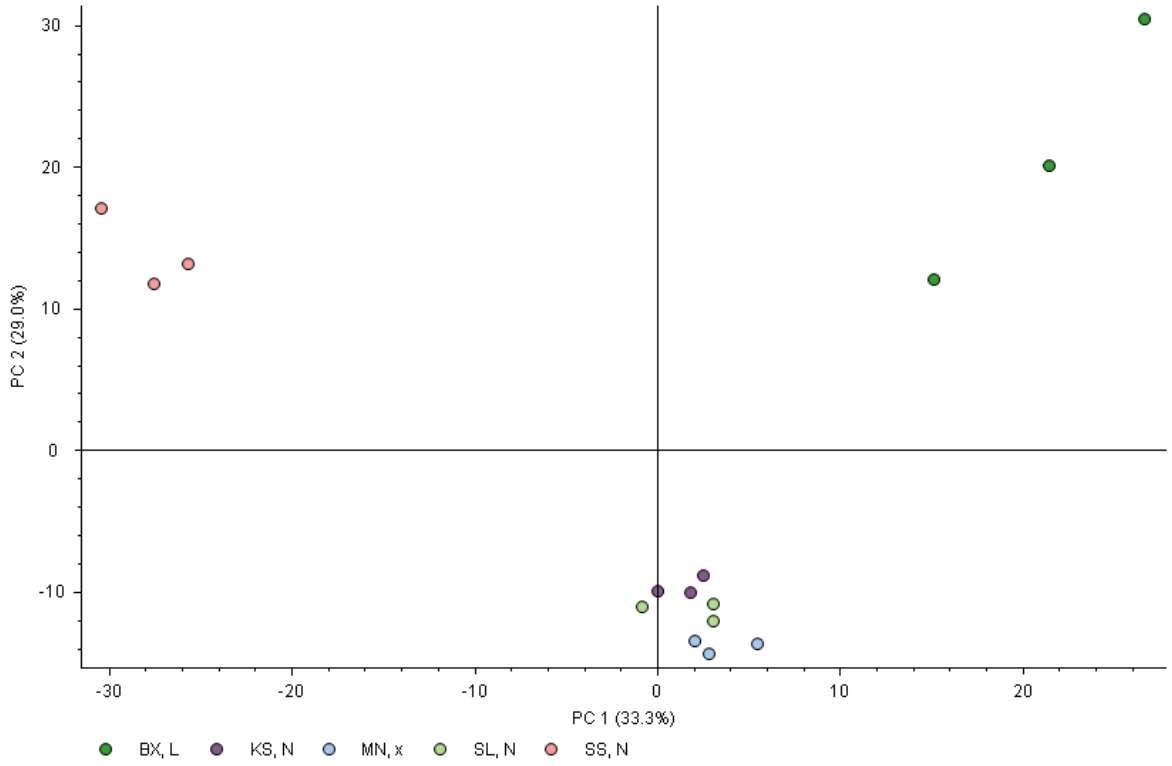

Figure 18 Comparison of different glove-leaching sample groups and three blank samples (MN, x) are shown within the present PCA plot. Feature filters were applied as described in the methods section above.

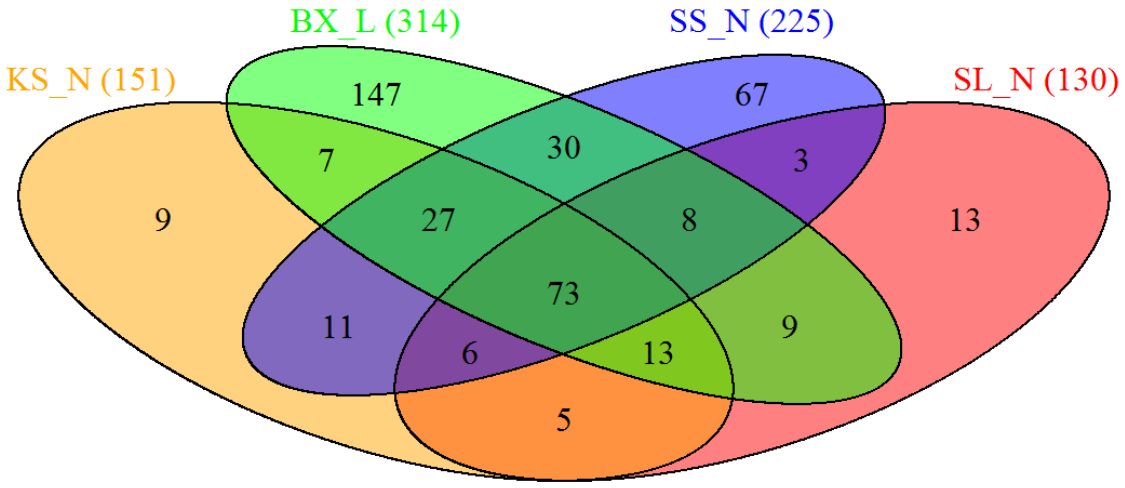

Figure 19 Venn diagram comparing the different investigated gloves. In order to be counted as present within a sample group features had to exceed an area intensity threshold of 1E4 counts*s^{-1} in each replicate and a group FV% of less than 50%. As all samples were prepared in MN-vials, features that were also found in all replicates of the sample group MN with a group FV% of less than 50% were not considered. The absolute amount of considered features per sample group is given in brackets next to each group label.

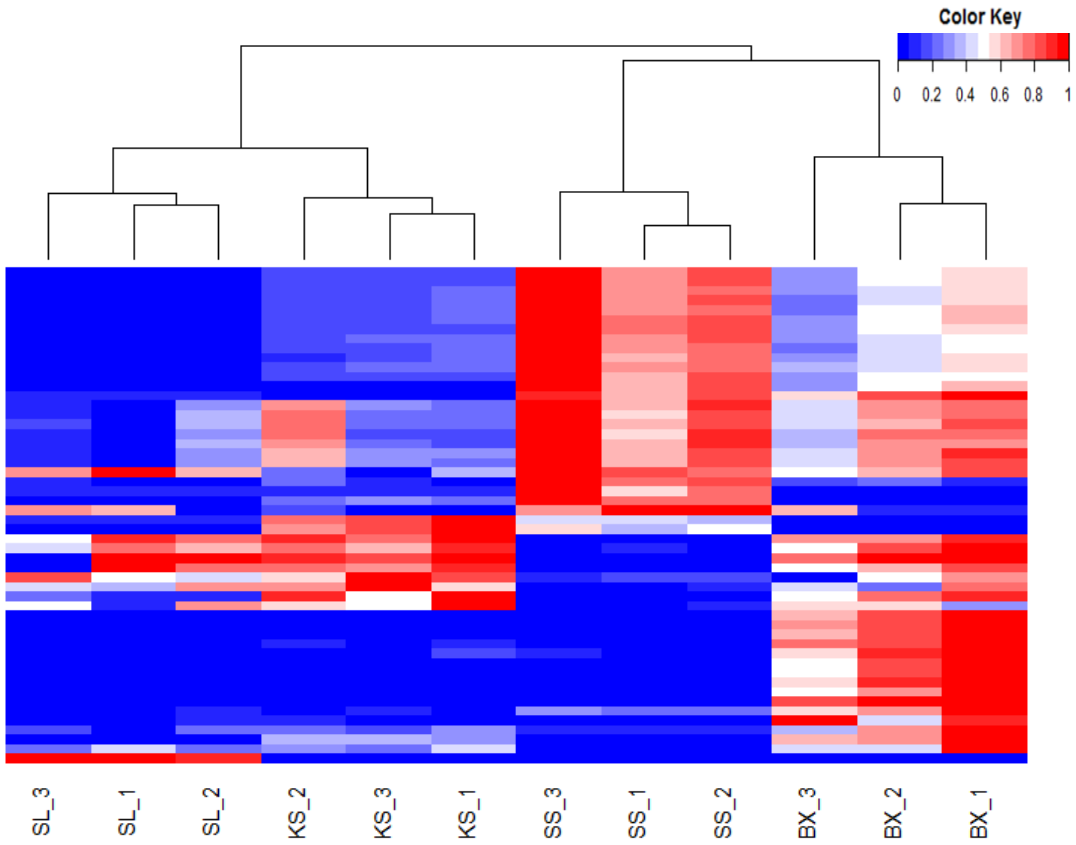

Figure 20 All 52 features (with signal intensities greater than 1E4) showing significant differences ($p_{adj} < 0.05$) between the vial-groups (according to a univariate ANOVA with a subsequent Tukey's range test) are compared sample wise within this heat map. Therefore the concentration range of each individual feature has been scaled to values between 0 and 1.

3.2.3 Pipet tips

Six different pipet tips (different vendors, volumes and colours) were tested for their leachable contaminants. In order to create a heat map (**Figure 21**) the same filters and statistical analyses as utilised for the glove comparisons were also applied here. From the dendrogram it can be seen that there were only one clearly distinguishable cluster formed by the sample groups E_20D and S_200G. Another formed cluster indicates the similarity between the blanks and E_200G. This implicates the hint that the according tips introduced only little contamination. Two other clusters can be imagined for S_1000B and E_1000D but they cannot be clearly distinguished from G_200D_1 and G_200D_1 & 3 respectively. The only contaminant identified in the process at MS2 level was Betaine. However, from **Figure 22** it can be seen that the main variance was not related to the formed sample groups, but to the measurement order. Hence, it can be concluded that the influence of the measurement sequence should be investigated in more detail in the future.

Table 10 Compounds identified within the different glove-leaching groups are given in this table. Identification was conducted via MS2 spectra comparison with mzCloud.

KS	SL	SS	BX
Triphenylphosphine oxide	Triphenylphosphine oxide	Triphenylphosphine oxide	Valine
PEG n7	PEG n6	PEG n7	Triphenylphosphine oxide
PEG n6	PEG n5	PEG n6	Trigonelline
PEG n5	Oleamide	PEG n5	Pyrogallol
N-Methylcaprolactam	Octadecanamine	Oleamide	Pirbuterol
Hexadecanamide	Hexadecanamide	N,N-Diisopropylethylamine	Phloroglucinol
Erucamide	Erucamide	Hexadecanamide	PEG n7
Diethyl phthalate	Diethyl phthalate	Erucamide	PEG n6
Dibutyl phthalate	Dibutyl phthalate	Diethyl phthalate	PEG n5
Decanamide	Decanamide	Dibutyl phthalate	Octadecanamine
Bis(2-ethylhexyl)adipate	Bis(2-ethylhexyl)adipate	Decanamide	N-Methylcaprolactam
2,2,6,6-Tetramethyl-4-piperidinol	2,2,6,6-Tetramethyl-4-piperidinol	Bis(2-ethylhexyl)adipate	N6,N6,N6-Trimethyl-L-lysine
12-Aminododecanoic acid	12-Aminododecanoic acid	Betaine	N,N-Diisopropylethylamine
		2-Mercaptobenzothiazole	Hexadecanamide
		2,2,6,6-Tetramethyl-4-piperidinol	Erucamide
		12-Aminododecanoic acid	DL-Carnitine
		1,3-Benzodioxolylbutanamine	Diethyl phthalate
			Dibutyl phthalate
			Decanamide
			Choline
			Buspirone
			Bis(2-ethylhexyl)adipate
			Betaine
			2,2,6,6-Tetramethyl-4-piperidinol
			12-Aminododecanoic acid
			1,3-Benzodioxolylbutanamine

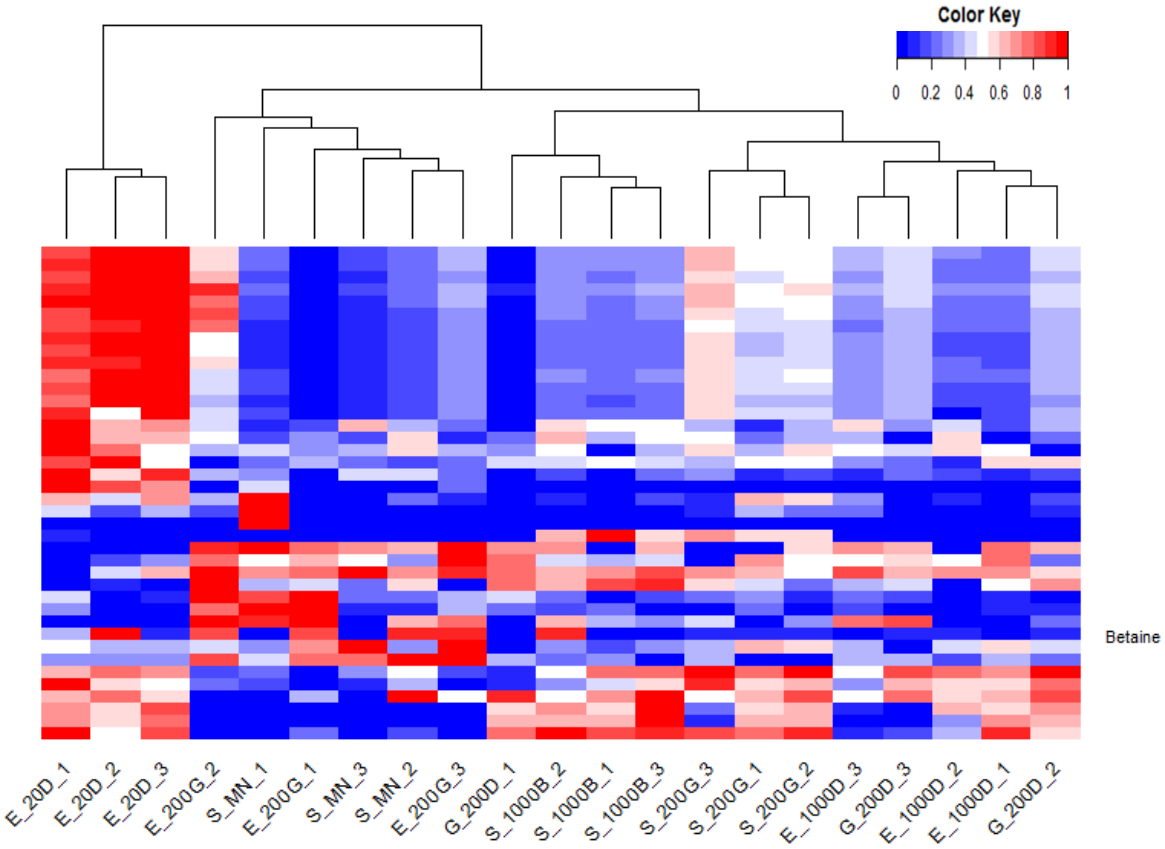

Figure 21 All 40 features (with signal intensities greater than 1E4) showing significant differences ($p_{adj} < 0.05$) between the pipet tip-groups (according to a univariate ANOVA with a subsequent Tukey's range test) are compared sample wise within this heat map. Therefore, the concentration range of each individual feature has been scaled to values between 0 and 1. The first letter is referring to the different vendors (Eppendorf (E), Star Lab (S) and Greiner Bio One (G)). Then the first number is giving the vendor-reported maximum volume of the tip in µL followed by a letter indicating the colour of the tip (transparent (D), yellow (G) and blue (B)). The last number is referring to the different replicates. Additionally, to the different pipet tips three blanks (S_MN_1-3) were added to the heat map.

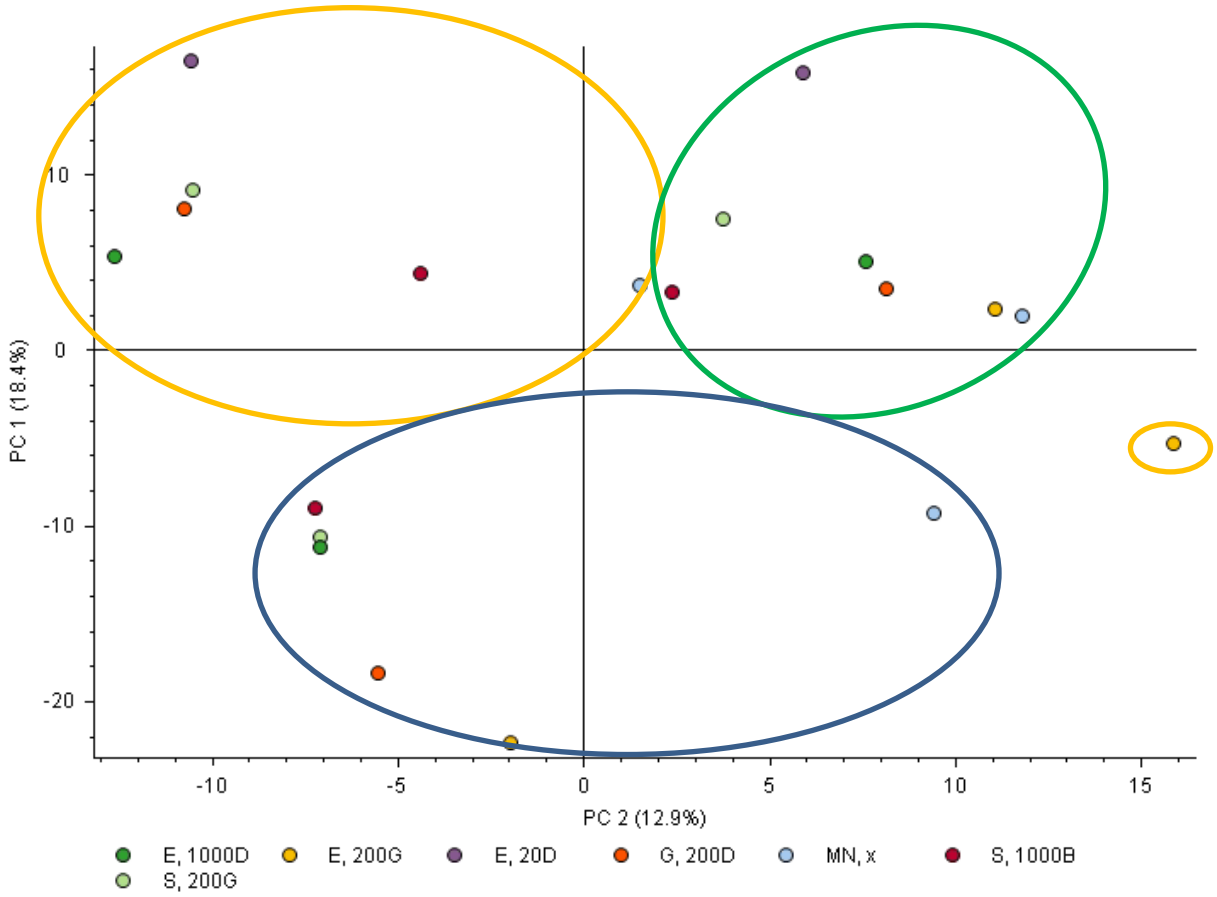

Figure 22 For the shown PCA scores plot only components that were present with an peak area of at least 1E4 signal intensity*s^{-1} in all replicates of at least one sample group with a compound coefficient of variance of less than 50% were considered. The first letter is referring to the different vendors (Eppendorf (E), Star Lab (S) and Greiner Bio One (G)). Then the number is giving the vendor-reported maximum volume of the different tips in µL followed by a letter indicating the colour of the tip (transparent (D), yellow (G) and blue (B)). Additionally to the different pipet tips three blanks (MN, x) were added. The circles are indicating in which third of the measurement sequence the samples were injected (first third (blue), second third (yellow) and last third (green)).

3.2.4 Plastic tubes and centrifuge tubes

For the comparisons between the differently prepared centrifuge tubes and plastic tubes similar results were obtained. The data pre-treatment was conducted in the same way as described for previous comparisons like gloves and pipet tips. As already observed and discussed for the pipet tip samples the main variation was not within the chosen sample groups but was related to the injection order (**Figure 23**). However, from the heat maps in **Figure 24** it can be seen that some features were significantly influenced by the conducted sample treatment. For the plastic tubes each sample group could be confirmed by the dendrogram. Moreover, the pattern observed there displayed an easily interpretable pattern. The uncleaned plastic tubes showed the highest intensities for most features presented in the heat map. On the other hand those washed with water showed decreased intensities and those washed with methanol and water even lower intensities and are most

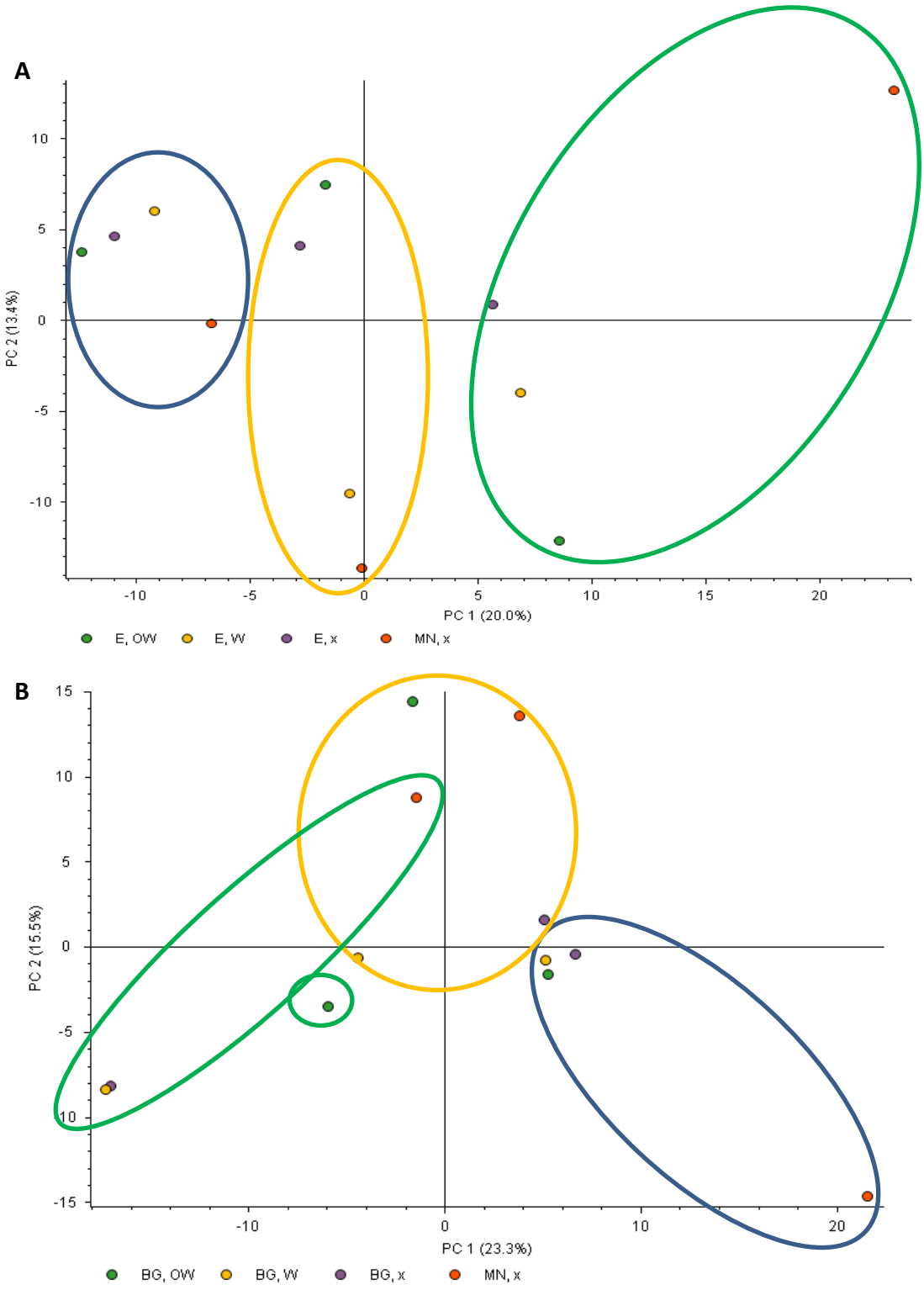

Figure 23 For the shown PCA scores plots only components that were present with an peak area of at least 1E4 signal intensity*s^{-1} in all replicates of at least one sample group with a compound coefficient of variance of less than 50% were considered. The first letter is referring to the different vendors (Bio One Greiner (BG), Eppendorf (E)). Then the sample pre-treatment is indicated (not washed (x), washed with water (W) or washed with methanol and water (OW)). Additionally to the different pipet tips three blanks (MN, x) were added. The circles are indicating in which third of the measurement sequence the samples were injected (first third (blue), second third (yellow) and last third (green)). In A the different plastic tube sample groups and in B the different centrifuge tube groups are shown.

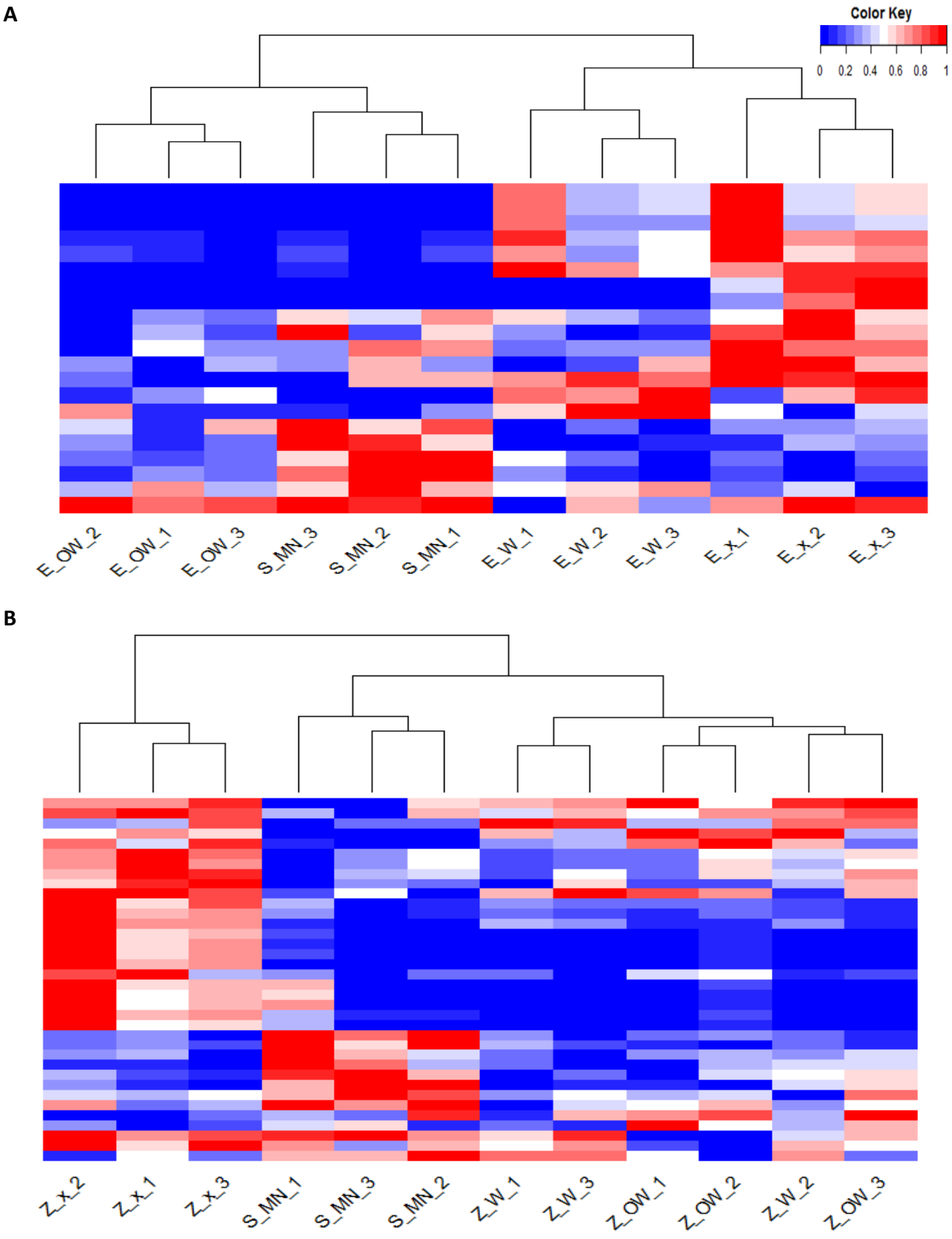

Figure 24 All features (with signal intensities greater than 1E4) which showed significant differences ($p_{adj} < 0.05$) between the investigated plastic tube groups (A) and centrifuge tube groups (B) (according to a univariate ANOVA with a subsequent Tukey's range test) are compared sample wise within this heat map. For A this was true for 21, for B for 36 features. For the heat map the concentration range of each individual feature has been scaled to values between 0 and 1. The first letter of the labels is indicating whether the sample was an plastic tube (E) or a centrifuge tube (Z). Then the sample pre-treatment is indicated (not washed (x), washed with water (W) or washed with methanol and water (OW)). Additionally to the different pipet tips three blanks (S_MN_1-3) were added.

similar to the blanks. However, the reasons for those features at the bottom of the heat map that showed an inverse pattern have not been investigated yet. A possible explanation would be an increase in intensity due to the decrease in intensity of those features that were washed out in the pre-treatment as described before. The very same effects could be observed for centrifuge tubes. However, additional washing with methanol did not have an influence on as many compounds as for the plastic tubes.

4 Conclusion

As a general conclusion it can be said that non-targeted data evaluation still needs further improvement. For example, evaluation tools reducing false positive peak reports (due to multiply integrated peaks or un-joined adducts or isotopes) need to be incorporated for easy use on a regular basis. Moreover, exclusion and inclusion lists with suspects (contaminants and analytes of interest respectively) should be established in order to improve run-to-run reproducibility and maximize the number of annotations. Regarding the cell culture experiments, an analytical workflow for the targeted analysis of most compounds of interest could be established. However, in order to draw biological conclusions the sample preparation (especially the filtration) still needs to be validated. Additionally, the uncertainty of the cell counts has to be improved so that significant changes can be found when different cell cultures are compared. Concerning the contamination experiments, the conclusion can be drawn that many materials influencing the background could be identified. In a possible next step, the influence of those contaminations on ion-suppression should be evaluated. Moreover, the meaningfulness of putting them on exclusion lists should be discussed and depending on the outcome such an exclusion list should be established.

5 List of abbreviations

Ala	Alanine
ANOVA	Analysis of variance
AOA	Ammonia oxidising archaea
AOB	Ammonia oxidising bacteria
Arg	Arginine
Asn	Asparagine
Asp	Aspartate
CD	Compound Discoverer 2.0
Cys	Cysteine
Ect	Ectoine
ESI	Electrospray ionisation
FDR	False discovery rate
FV%	Feature coefficient of variance
Glt	Glutamate
Glu	Glutamine
Gly	Glycine
H_0	Null hypothesis
Hec	Hydroxyectoine
His	Histidine
HPLC	High performance liquid chromatography
IC	Ion-exchange chromatography
Ile	Isoleucine
LC	Liquid chromatography
LCP	Lowest calibration point
Leu	Leucine
LOQ	Limit of quantification
Lys	Lysine
MCS	Multi-component standard
Met	Methionine
MS	Mass spectrometry

PCA	Principal component analysis
Phe	Phenylalanine
Pro	Proline
Pyr	Pyruvate
qPCR	Quantitative polymerase chain reaction
RP	Reversed phase
RT	Retention time
Ser	Serine
Thr	Threonine
TIC	Total ion chromatogram
Trp	Tryptophan
Tukey HSD	Tukey's honest significant difference
Tyr	Tyrosine
Val	Valine
VD	Venn diagram

6 References

Almeida, A. M., Castel-Branco, M. M., and Falcão, A. C. (2002). Linear regression for calibration lines revisited: weighting schemes for bioanalytical methods. *J. Chromatogr. B* 774, 215–222. doi:10.1016/S1570-0232(02)00244-1.

Anggard, E., and Sedvall, G. (1969). Gas chromatography of catecholamine metabolites using electron capture detection and mass spectrometry. *Anal. Chem.* 41, 1250–1256. doi:10.1021/ac60279a042.

B. Dunn, W., C. Bailey, N. J., and E. Johnson, H. (2005). Measuring the metabolome: current analytical technologies. *Analyst* 130, 606–625. doi:10.1039/B418288J.

Benjamini, Y., and Hochberg, Y. (1995). Controlling the False Discovery Rate: A Practical and Powerful Approach to Multiple Testing. *J. R. Stat. Soc. Ser. B Methodol.* 57, 289–300.

Bollmann, A., Sedlacek, C. J., Norton, J., Laanbroek, H. J., Suwa, Y., Stein, L. Y., et al. (2013). Complete genome sequence of Nitrosomonas sp. Is79, an ammonia oxidizing bacterium adapted to low ammonium concentrations. *Stand. Genomic Sci.* 7, 469–482. doi:10.4056/sigs.3517166.

Broadhurst, D. I., and Kell, D. B. (2006). Statistical strategies for avoiding false discoveries in metabolomics and related experiments. *Metabolomics Heidelb.* 2, 171–196. doi:http://dx.doi.org/10.1007/s11306-006-0037-z.

Clark, C., and Schmidt, E. L. (1967). Growth Response of Nitrosomonas europaea to Amino Acids. *J. Bacteriol.* 93, 1302–1308.

Conover, W. J. (1999). *Practical nonparametric statistics*. Wiley.

Daims, H., Lebedeva, E. V., Pjevac, P., Han, P., Herbold, C., Albertsen, M., et al. (2015). Complete nitrification by Nitrospira bacteria. *Nature* 528, 504–509. doi:10.1038/nature16461.

DeFelice, B. C., Mehta, S. S., Samra, S., Čajka, T., Wancewicz, B., Fahrmann, J. F., et al. (2017). Mass Spectral Feature List Optimizer (MS-FLO): A Tool To Minimize False Positive Peak

Reports in Untargeted Liquid Chromatography–Mass Spectroscopy (LC-MS) Data Processing. *Anal. Chem.* 89, 3250–3255. doi:10.1021/acs.analchem.6b04372.

Dettmer, K., Aronov, P. A., and Hammock, B. D. (2007). Mass spectrometry-based metabolomics. *Mass Spectrom. Rev.* 26, 51–78. doi:10.1002/mas.20108.

Doxey, A. C., Kurtz, D. A., Lynch, M. D., Sauder, L. A., and Neufeld, J. D. (2015). Aquatic metagenomes implicate Thaumarchaeota in global cobalamin production. *ISME J.* 9, 461–471. doi:10.1038/ismej.2014.142.

Editors, L. The Secrets of Electrospray Ionization: Why Less is More. Available at: http://www.chromatographyonline.com/secrets-electrospray-ionization-why-less-more-0 [Accessed January 6, 2017].

Fiehn, O. (2001). Combining Genomics, Metabolome Analysis, and Biochemical Modelling to Understand Metabolic Networks. *Int. J. Genomics* 2, 155–168. doi:10.1002/cfg.82.

Fiehn, O. (2002). Metabolomics – the link between genotypes and phenotypes. *Plant Mol. Biol.* 48, 155–171. doi:10.1023/A:1013713905833.

Fiehn, O., Kopka, J., Dörmann, P., Altmann, T., Trethewey, R. N., and Willmitzer, L. (2000a). Metabolite profiling for plant functional genomics. *Nat. Biotechnol.* 18, 1157–1161. doi:10.1038/81137.

Fiehn, O., Kopka, J., Trethewey, R. N., and Willmitzer, L. (2000b). Identification of uncommon plant metabolites based on calculation of elemental compositions using gas chromatography and quadrupole mass spectrometry. *Anal. Chem.* 72, 3573–3580. doi:10.1021/ac991142i.

Franceschi, P., Giordan, M., and Wehrens, R. (2013). Multiple comparisons in mass-spectrometry-based -omics technologies. *TrAC Trends Anal. Chem.* 50, 11–21. doi:10.1016/j.trac.2013.04.011.

Frijlink, M. J., Abee, T., Laanbroek, H. J., Boer, W. de, and Konings, W. N. (1992). Secondary transport of amino acids in Nitrosomonas europaea. *Arch. Microbiol.* 157, 389–393. doi:10.1007/BF00248686.

G. Marshall, A., T. Blakney, G., Chen, T., K. Kaiser, N., M. McKenna, A., P. Rodgers, R., et al. (2013). Mass Resolution and Mass Accuracy: How Much Is Enough? *Mass Spectrom.* 2. doi:10.5702/massspectrometry.S0009.

Hatzenpichler, R., Lebedeva, E. V., Spieck, E., Stoecker, K., Richter, A., Daims, H., et al. (2008). A moderately thermophilic ammonia-oxidizing crenarchaeote from a hot spring. *Proc. Natl. Acad. Sci.* 105, 2134–2139. doi:10.1073/pnas.0708857105.

Kim, J.-G., Park, S.-J., Sinninghe Damsté, J. S., Schouten, S., Rijpstra, W. I. C., Jung, M.-Y., et al. (2016). Hydrogen peroxide detoxification is a key mechanism for growth of ammonia-oxidizing archaea. *Proc. Natl. Acad. Sci. U. S. A.* 113, 7888–7893. doi:10.1073/pnas.1605501113.

Kind, T., and Fiehn, O. (2006). Metabolomic database annotations via query of elemental compositions: Mass accuracy is insufficient even at less than 1 ppm. *BMC Bioinformatics* 7, 234. doi:10.1186/1471-2105-7-234.

Kind, T., and Fiehn, O. (2007). Seven Golden Rules for heuristic filtering of molecular formulas obtained by accurate mass spectrometry. *BMC Bioinformatics* 8, 105. doi:10.1186/1471-2105-8-105.

Könneke, M., Bernhard, A. E., de la Torre, J. R., Walker, C. B., Waterbury, J. B., and Stahl, D. A. (2005). Isolation of an autotrophic ammonia-oxidizing marine archaeon. *Nature* 437, 543–546. doi:10.1038/nature03911.

Lawson, T. N., Weber, R. J. M., Jones, M. R., Chetwynd, A. J., Rodríguez-Blanco, G., Di Guida, R., et al. (2017). msPurity: Automated Evaluation of Precursor Ion Purity for Mass Spectrometry-Based Fragmentation in Metabolomics. *Anal. Chem.* doi:10.1021/acs.analchem.6b04358.

Lebedeva, E. V., Hatzenpichler, R., Pelletier, E., Schuster, N., Hauzmayer, S., Bulaev, A., et al. (2013). Enrichment and Genome Sequence of the Group I.1a Ammonia-Oxidizing Archaeon "Ca. Nitrosotenuis uzonensis" Representing a Clade Globally Distributed in Thermal Habitats. *PLOS ONE* 8, e80835. doi:10.1371/journal.pone.0080835.

Lehmann, W. D. (2017). A timeline of stable isotopes and mass spectrometry in the life sciences. *Mass Spectrom. Rev.* 36, 58–85. doi:10.1002/mas.21497.

Magnusson, B. and Örnemark, U. (eds.) Eurachem Guide: The Fitness for Purpose of Analytical Methods – A Laboratory Guide to Method Validation and Related Topics, (2nd ed. 2014). ISBN 978-91-87461-59-0. Available from http://www.eurachem.org.

Marshall, A. G., Hendrickson, C. L., and Shi, S. D.-H. (2002). Peer Reviewed: Scaling MS Plateaus with High-Resolution FT-ICRMS. *Anal. Chem.* 74, 252 A-259 A. doi:10.1021/ac022010j.

Neubauer, S., Haberhauer-Troyer, C., Klavins, K., Russmayer, H., Steiger, M. G., Gasser, B., et al. (2012a). U13C cell extract of Pichia pastoris – a powerful tool for evaluation of sample preparation in metabolomics. *J. Sep. Sci.* 35, 3091–3105. doi:10.1002/jssc.201200447.

Neubauer, S., Haberhauer-Troyer, C., Klavins, K., Russmayer, H., Steiger, M. G., Gasser, B., et al. (2012b). U13C cell extract of Pichia pastoris – a powerful tool for evaluation of sample preparation in metabolomics. *J. Sep. Sci.* 35, 3091–3105. doi:10.1002/jssc.201200447.

Noury, S., Silvi, B., and Gillespie, R. J. (2002). Chemical Bonding in Hypervalent Molecules: Is the Octet Rule Relevant? *Inorg. Chem.* 41, 2164–2172. doi:10.1021/ic011003v.

Oliver, S. G., Winson, M. K., Kell, D. B., and Baganz, F. (1998). Systematic functional analysis of the yeast genome. *Trends Biotechnol.* 16, 373–378. doi:10.1016/S0167-7799(98)01214-1.

Ortmayr, K., Causon, T. J., Hann, S., and Koellensperger, G. (2016). Increasing selectivity and coverage in LC-MS based metabolome analysis. *TrAC Trends Anal. Chem.* 82, 358–366. doi:10.1016/j.trac.2016.06.011.

Ortmayr, K., Schwaiger, M., Hann, S., and Koellensperger, G. (2015). An integrated metabolomics workflow for the quantification of sulfur pathway intermediates employing thiol protection with N -ethyl maleimide and hydrophilic interaction liquid chromatography tandem mass spectrometry. *Analyst* 140, 7687–7695. doi:10.1039/C5AN01629K.

Palatinszky, M., Herbold, C., Jehmlich, N., Pogoda, M., Han, P., von Bergen, M., et al. (2015). Cyanate as an energy source for nitrifiers. *Nature* 524, 105–108. doi:10.1038/nature14856.

Preez, I. du, Luies, L., and Loots, D. T. (2017). Metabolomics biomarkers for tuberculosis diagnostics: current status and future objectives. *Biomark. Med.* 11, 179–194. doi:10.2217/bmm-2016-0287.

Rainville, P. D., Theodoridis, G., Plumb, R. S., and Wilson, I. D. (2014). Advances in liquid chromatography coupled to mass spectrometry for metabolic phenotyping. *TrAC Trends Anal. Chem.* 61, 181–191. doi:10.1016/j.trac.2014.06.005.

Ranninger, C., Schmidt, L. E., Rurik, M., Limonciel, A., Jennings, P., Kohlbacher, O., et al. (2016). Improving global feature detectabilities through scan range splitting for untargeted metabolomics by high-performance liquid chromatography-Orbitrap mass spectrometry. *Anal. Chim. Acta* 930, 13–22. doi:10.1016/j.aca.2016.05.017.

Rhoades, S. D., and Weljie, A. M. (2016). Comprehensive optimization of LC–MS metabolomics methods using design of experiments (COLMeD). *Metabolomics* 12, 183. doi:10.1007/s11306-016-1132-4.

Rodionov, D. A., Vitreschak, A. G., Mironov, A. A., and Gelfand, M. S. (2003). Comparative Genomics of the Vitamin B12 Metabolism and Regulation in Prokaryotes. *J. Biol. Chem.* 278, 41148–41159. doi:10.1074/jbc.M305837200.

Roy, S. M., Anderle, M., Lin, H., and Becker, C. H. (2004). Differential expression profiling of serum proteins and metabolites for biomarker discovery. *Int. J. Mass Spectrom.* 238, 163–171. doi:10.1016/j.ijms.2004.03.017.

Sañudo-Wilhelmy, S. A., Gómez-Consarnau, L., Suffridge, C., and Webb, E. A. (2014). The Role of B Vitamins in Marine Biogeochemistry. *Httpdxdoiorg101146annurev-Mar.-120710-100912*. Available at: http://www.annualreviews.org/doi/10.1146/annurev-marine-120710-100912 [Accessed March 14, 2017].

Schwartz, M. A., Bommer, P., and Vane, F. M. (1967). Diazepam metabolites in the rat: Characterization by high-resolution mass spectrometry and nuclear magnetic resonance. *Arch. Biochem. Biophys.* 121, 508–516. doi:10.1016/0003-9861(67)90106-3.

Sedlacek, C. J., Nielsen, S., Greis, K. D., Haffey, W. D., Revsbech, N. P., Ticak, T., et al. (2016). Effects of Bacterial Community Members on the Proteome of the Ammonia-Oxidizing

Bacterium Nitrosomonas sp. Strain Is79. *Appl. Environ. Microbiol.* 82, 4776–4788. doi:10.1128/AEM.01171-16.

Shellie, R. A., Welthagen, W., Zrostliková, J., Spranger, J., Ristow, M., Fiehn, O., et al. (2005). Statistical methods for comparing comprehensive two-dimensional gas chromatography–time-of-flight mass spectrometry results: Metabolomic analysis of mouse tissue extracts. *J. Chromatogr. A* 1086, 83–90. doi:10.1016/j.chroma.2005.05.088.

Sumner, L. W., Amberg, A., Barrett, D., Beale, M. H., Beger, R., Daykin, C. A., et al. (2007). Proposed minimum reporting standards for chemical analysis Chemical Analysis Working Group (CAWG) Metabolomics Standards Initiative (MSI). *Metabolomics Off. J. Metabolomic Soc.* 3, 211–221. doi:10.1007/s11306-007-0082-2.

Taylor, J., King, R. D., Altmann, T., and Fiehn, O. (2002). Application of metabolomics to plant genotype discrimination using statistics and machine learning. *Bioinformatics* 18, S241–S248. doi:10.1093/bioinformatics/18.suppl_2.S241.

Theodoridis, G., Gika, H. G., and Wilson, I. D. (2011). Mass spectrometry-based holistic analytical approaches for metabolite profiling in systems biology studies. *Mass Spectrom. Rev.* 30, 884–906. doi:10.1002/mas.20306.

Tukey, J. W. (1949). Comparing Individual Means in the Analysis of Variance. *Biometrics* 5, 99–114. doi:10.2307/3001913.

Yanes, O., Tautenhahn, R., Patti, G. J., and Siuzdak, G. (2011). Expanding Coverage of the Metabolome for Global Metabolite Profiling. *Anal. Chem.* 83, 2152–2161. doi:10.1021/ac102981k.